



UNIVERSITEIT VAN PRETORIA
UNIVERSITY OF PRETORIA
YUNIBESITHI YA PRETORIA

Denkleiers • Leading Minds • Dikgopolo tša Dihlalefi

Antifungal mode of action studies of an antimicrobial peptide, Os, in planktonic *Candida albicans* (ATCC 90028).

by

Dalton Charl Moller

Student number: 04667124

Supervisor: Prof. A.R.M. Gaspar

Co-supervisors: Prof. M.J. Bester, Dr H. Taute

Submitted in partial fulfilment of the degree:

MSc (Magister Scientiae) in Biochemistry,

Department of Biochemistry, Genetics and Microbiology

in the Faculty of Natural and Agricultural Sciences

University of Pretoria

08 May 2020

DECLARATION OF ORIGINALITY UNIVERSITY OF PRETORIA

The Department of Biochemistry, genetics and microbiology places great emphasis upon integrity and ethical conduct in the preparation of all written work submitted for academic evaluation.

While academic staff teaches you about referencing techniques and how to avoid plagiarism, you too have a responsibility in this regard. If you are at any stage uncertain as to what is required, you should speak to your lecturer before any written work is submitted.

You are guilty of plagiarism if you copy something from another author's work (e.g. a book, an article or a website) without acknowledging the source and pass it off as your own. In effect, you are stealing something that belongs to someone else. This is not only the case when you copy work word-for-word (verbatim), but also when you submit someone else's work in a slightly altered form (paraphrase) or use a line of argument without acknowledging it. You are not allowed to use work previously produced by another student. You are also not allowed to let anybody copy your work with the intention of passing it off as his/her work.

Students who commit plagiarism will not be given any credit for plagiarised work. The matter may also be referred to the Disciplinary Committee (Students) for a ruling. Plagiarism is regarded as a serious contravention of the University's rules and can lead to expulsion from the University.

The declaration which follows must accompany all written work submitted while you are a student of the Department of Biochemistry, Genetics, and Microbiology. No written work will be accepted unless the declaration has been completed and attached.

Full names of student: Dalton Charl Moller


Student number: 04667124

Topic of work: MSc dissertation

Declaration

1. I understand what plagiarism is and am aware of the University's policy in this regard.
2. I declare that this proposal (e.g. essay, report, project, assignment, dissertation, thesis, etc) is my own original work. Where other people's work has been used (either from a printed source, Internet or any other source), this has been properly acknowledged and referenced in accordance with departmental requirements.
3. I have not used work previously produced by another student or any other person to hand in as my own.
4. I have not allowed, and will not allow, anyone, to copy my work with the intention of passing it off as his or her own work.

SIGNATURE



.....

Acknowledgements

The completion of this study required the support and knowledge of a lot of different people. I want to take this opportunity to thank all of them and acknowledge their contributions, big or small.

- I first and foremost want to thank my supervisor, Prof. A.R.M. Gaspar, for all her support, teachings and guidance. She always prioritises her students and motivates us to work to the best of our abilities.
- Thank you to my co-supervisors, Prof. M.J. Bester and Dr H Taute, for teaching me something new every day. Prof. Bester constantly motivates her students and helps them reach their full potential. Thank you Dr. Taute for all the early mornings and late afternoons, teaching me the necessary skills to complete this project.
- I want to thank my family and friends for all their support and motivation. A special thanks to Lizane Jordaan for helping me with the writing process of this project and for the constant moral support throughout my studies. I want to thank my parents in particular for their constant emotional and financial support. They have always encouraged me to follow my own path and pursue the field of science.
- Thank you to all the members of the Biotherapeutics research group and the help they provided. We make it a priority in our group to help each other and share our knowledge. I also want to thank the Cell Biology group, working in collaboration with the Biotherapeutics group. It can sometimes feel like a second family.
- I want to give a special thanks to our lab manager, Sandra van Wyngaardt, who always goes the extra mile to help students in the laboratory. Her kindness and support keep all of us going.
- Thank you to the team at the Laboratory for Microscopy and Microanalysis at the University of Pretoria, not only for the technical support, but also for the knowledge and skills provided for this study.
- Thank you to Dr. B. Mans for the help with isothermal titration calorimetry. He provided the equipment, as well as the knowledge to complete this part of the study. His insights and advice were invaluable.
- Thank you to Prof. C. Durant for the advice and assistance with the flow cytometry experiments in this study, as well as providing the necessary equipment to allow for these experiments.

- Finally, thank you to the University of Pretoria, the National Research Foundation and the Department of Biochemistry, Genetics and Microbiology for providing the funding, space and equipment needed to complete this study.

Table of Contents

DECLARATION OF ORIGINALITY UNIVERSITY OF PRETORIA	i
Acknowledgements.....	ii
Table of Contents	iv
List of abbreviations.....	vi
List of Figures	viii
List of Tables	x
Summary	xi
1 Literature review	1
1.1 <i>Candida albicans</i>	1
1.1.1 Antibiotic resistance.....	1
1.2 Antimicrobial peptides.....	2
1.2.1 Leads for novel antimicrobial agents.....	2
1.2.2 Modes of action	6
1.3 Methods for determining the mechanisms of action of AMPs.....	10
1.4 Background to the study	11
1.5 Aim of the study.....	14
1.5.1 Objectives.....	14
2 Methodology	15
2.1 Overview	15
2.2 Chemical reagents.....	16
2.3 Synthesis of peptides and preparation of peptide solutions.....	16
2.4 Anti-planktonic microbroth dilution assay	16
2.4.1 Cell viability	18
2.5 Coated glass coverslip preparation.....	19
2.6 Scanning electron microscopy	19
2.7 Transmission electron microscopy.....	21
2.8 Isothermal titration calorimetry	23
2.9 Cell wall components binding assay	24
2.10 Membrane depolarization assay	24

2.11	Intracellular co-localisation of FAM-Os and vacuole staining	25
2.12	Statistical analysis	28
3	Results	29
3.1	Modified microbroth dilution assay.....	29
3.2	Inhibitory activity of Os.....	29
3.3	Effect of Os on <i>C. albicans</i> ultrastructure.....	31
3.4	Interactions with cell wall components	36
3.5	Membrane depolarization	38
3.6	Intracellular localisation	39
4	Discussion	43
5	Conclusion and future perspectives	51
6	References	54

List of abbreviations

β GRP	β -glucan recognition protein
5-FAM	5-Carboxyfluorescein

A

AFPs	Antifungal peptides
AMPs	Antimicrobial peptides

C

<i>C. albicans</i>	<i>Candida albicans</i>
CaCO ₃	Calcium carbonate
CBM	Carbohydrate-binding modules
CLSM	Confocal laser scanning microscopy
CTB	CellTiter Blue
CTB-CMAC	CellTracker Blue-CMAC

D

ddH ₂ O	Double distilled water
DiBAC ₄ (3)	Bis-(1,3-dibutylbarbituric acid) trimethine oxonol
DIC	Differential interference Contrast

E

EDTA	Ethylenediaminetetraacetic acid
Em	Emission wavelength
EV	Extracellular vesicles
Ex	Excitation wavelength

H

HMDS	Hexamethyldisilazane
------	----------------------

I

IC ₅₀	Concentration inhibiting 50% growth
ICU	Intensive care unit
ISE	Ion selective electrode
ITC	Isothermal titration calorimetry

M

MDR	Multi-drug resistant
MFC	Minimum fungicidal concentration
MIC	Minimum inhibitory concentration
MOPS	3-(<i>N</i> -morpholino) propanesulfonic acid

N

NaP	Sodium phosphate buffer
-----	-------------------------

O

OsO ₄	Osmium tetroxide
------------------	------------------

P

PBS	Phosphate-buffered saline
-----	---------------------------

R

RDA	Radial diffusion assay
ROS	Reactive oxygen species
RPMI	Roswell Park Memorial Institute 1640 growth medium

S

SEM	Scanning electron microscopy
-----	------------------------------

T

TEM	Transmission electron microscopy
-----	----------------------------------

Y

YPD	Yeast peptone dextrose
-----	------------------------

List of Figures

Figure 1.1: Three common mechanisms of resistance in <i>C. albicans</i> .	2
Figure 1.2: The four structural classifications of AMPs.	3
Figure 1.3: Simplified representation of the structure of the cell wall of <i>C. albicans</i> .	6
Figure 1.4: Different models for membrane permeabilization by antimicrobial peptides.	7
Figure 1.5: A representation of a cell membrane containing membrane proteins responsible for maintaining an electrostatic potential across the membrane.	8
Figure 1.6: Convergent membrane trafficking involving the pathways for vacuole protein sorting, endocytosis, autophagy and vacuole inheritance in budding yeast.	9
Figure 1.7: Intracellular distribution of pVEC in <i>C. albicans</i> at different peptide concentrations.	10
Figure 2.1: An overview of the methodology and the different techniques used in the study.	15
Figure 2.2: The chemical structure of resazurin, the chemical used in CellTiter Blue staining.	18
Figure 2.3: Chemical structure of the monomer unit of poly-L-lysine.	19
Figure 2.4: (A) The different components and layout of a scanning electron microscope.	20
Figure 2.5: A diagram depicting the different components of a transmission electron microscope and showing how the electron beam is directed to interact with the tissue and to create an image.	22
Figure 2.6: Chemical structures of cell wall components, mannan (left) and laminarin (right) found in <i>C. albicans</i> cell walls. Drawn using Chems sketch.	23
Figure 2.7: The chemical structure of protonated bis-(1,3-dibutylbarbituric acid) trimethine oxonol [DiBAC ₄ (3)].	24
Figure 3.1: Fluorescence as a measure of the viability of planktonic <i>C. albicans</i> cells grown in different dilutions of RPMI/NaP with/without 2.5 μ M AmpB.	29
Figure 3.2: The activity of (A) AmpB (positive control), (B) Os and (C) melittin against planktonic <i>C. albicans</i> cells after 3 hours treatment determined with the modified microbroth dilution assay.	30

Figure 3.3: Scanning electron microscope images of planktonic *C. albicans* treated for 3 hours with AmpB or Os at concentrations equal to the IC₂₅, IC₅₀ and IC₇₅. 32

Figure 3.4: Transmission electron microscope images at different magnifications of planktonic *C. albicans* cells treated with different concentrations of AmpB. 34

Figure 3.5: Transmission electron microscope images of planktonic *C. albicans* cells treated at the IC₂₅, IC₅₀ and IC₇₅ of Os. 35

Figure 3.6: Titration graphs indicating heat changes from mannan or laminarin mixed with buffer and EDTA interacting with CaCO₃ respectively. 36

Figure 3.7: Titration graphs indicating heat changes due to interactions between Os and mannan and laminarin respectively. 37

Figure 3.8: The amount of membrane depolarization caused by different concentrations (0.15-10 μM) of (A) melittin and (B) Os in *C. albicans* membranes. 39

Figure 3.9: Scatterplot graphs of 5-FAM peptide and CTB-CMAC fluorescent signals obtained from flow cytometry. 40

Figure 3.10: Percentage of total cells containing either CTB-CMAC or 5-FAM measured using flow cytometry for *C. albicans* cells treated with fluorescently labelled peptides. 41

Figure 3.11: CLSM images of planktonic *C. albicans* cells stained with CellTracker Blue and treated with free 5-FAM and peptides (penetratin or Os) labelled with 5-FAM. 42

Figure 4.1: A model of activity of AmpB towards *C. albicans*. 45

List of Tables

Table 1.1: Reported peptides and peptidomimetics in commercial development.	5
Table 1.2: The original peptide and the Os derivative along with their sequences, lengths, mass and charge at physiological pH.	12
Table 1.3: Properties of Os identified in previous studies.....	13
Table 2.1: The different concentrations of Os used in ITC with the corresponding concentrations of laminarin and mannan used as titrant.	24
Table 3.1: The IC ₂₅ , IC ₅₀ and IC ₇₅ of AmpB and Os against <i>C. albicans</i> growth.	30
Table 3.2: Inhibitory activity of Os and AmpB at their respective IC ₅₀ values against planktonic <i>C. albicans</i> in the presence of increasing concentrations of mannan and laminarin.	38

Summary

Candida albicans is a fungus found in the normal biota of humans, but in immuno-compromised individuals, *C. albicans* forms complex biofilms on the surface of medical prosthetics, skin, oral cavities, the urinary tract, and other epithelial cell layers. Biofilms and the development of drug resistance has limited treatment options. Antimicrobial peptides (AMPs) are increasingly becoming attractive therapeutic agents for the treatment of these infections due to their multifunctional properties, multiple cellular targets, and the lower incidence of resistance development.

Previous studies have shown that Os, an AMP derived from the tick defensin OsDef2, has antifungal activity against *C. albicans*. Preliminary antifungal mode of action studies indicated that Os induces the formation of reactive oxygen species although not a primary mode of killing. Os causes membrane permeabilization, which is inhibited by an excess of free laminarin and mannan. Furthermore, Os was shown to bind plasmid DNA but was inactive in high salt conditions.

The aim of this study was to further explore the mode of action of Os in planktonic *C. albicans* (ATCC 90028) cells. A modified microbroth dilution assay was developed to allow rapid screening of salt sensitive AMPs such as Os. With this method the IC₅₀ of the positive control, amphotericin B (AmpB), and Os were determined as $0.547 \pm 0.056 \mu\text{M}$ and $1.163 \pm 0.116 \mu\text{M}$, respectively.

The effects of AmpB and Os on cellular morphology were evaluated using scanning electron microscopy and transmission electron microscopy at their respective IC₂₅, IC₅₀ and IC₇₅ values. When comparing the effects of Os with AmpB on the cell wall and membrane, Os had more severe and non-specific effects. Os induced the formation of pits on the cell surface and pores in the cell membrane, as well as increased budding scars.

Using isothermal titration calorimetry, no interaction between Os and the fungal cell wall components, mannan and laminarin, could be detected. Factors such as the lack of tryptophan and aspartate residues as well as β -sheet secondary structures may account for the lack of interaction. However, with the modified microbroth dilution assay in the presence of excess of mannan or laminarin (20 mg/mL), reduced activity from Os was observed. The formation of soluble macro-complexes between Os and the cell wall components at high concentrations may account for reduced activity.

The ability of Os to cause membrane depolarization was evaluated with bis-(1,3-dibutylbarbituric acid) trimethine oxonol. The control, melittin, caused a linear increase in depolarization with a significant increase at $0.63 \mu\text{M}$, while Os caused a sigmoidal increase in depolarization with a significant increase at $2.5 \mu\text{M}$. Therefore, membrane depolarization occurs following membrane permeabilization which occurs at $2 \mu\text{M}$.

Finally, the localisation of $0.5 \mu\text{M}$ and $6.4 \mu\text{M}$ (IC₂₅, IC₇₅) 5-FAM-Os, and concurrently the effect on vacuoles loaded with CellTracker Blue-CMAC, was determined with flow cytometry and confocal laser

scanning microscopy (CLSM). Findings were that Os, at a concentration below its IC_{50} , binds to the cell membrane, then translocates and binds DNA. At a concentration above its IC_{50} , Os accumulates in the cytoplasm and causes destruction of membranes, including that of vacuoles, leading to cell death.

In conclusion, this study shows that Os is a membrane acting AMP that can be further developed for clinical application as an antifungal drug.

1 Literature review

1.1 *Candida albicans*

Candida albicans is a multiform fungus (able to form yeast and hyphal cells) and is the most prevalent fungal species in the human microbiome. A compromised immune system, stress and other microbial infections can cause an overgrowth of *C. albicans* leading to a wide range of infections. Premature infants or the aged are at the greatest risk for infection while other risk factors include a prolonged stay in an intensive care unit (ICU), renal failure and/or prolonged exposure to broad-spectrum antimicrobial agents (Pfaller and Diekema, 2007). The biggest challenge is the ability of *Candida* to form biofilms on surfaces, such as catheters or prosthetics. Biofilms are dense cell communities with a protective extracellular matrix that increases the organism's resistance to drug treatment (Nobile and Johnson, 2015).

1.1.1 Antibiotic resistance

Misuse of antibiotics and the development of resistance is due to unnecessary usage, and includes the use of antibiotics to increase the growth of farm animals, prolonged exposure to antibiotics at levels lower than the effective dose, the sharing of prescribed antibiotics and the unnecessary prescription of antibiotics (Levy, 2002).

Over the years, multiple different resistant strains of *C. albicans* have arisen, rendering conventional antifungals, such as amphotericin B (AmpB), ineffective. *C. albicans* can form biofilms, resulting in the development of antimicrobial resistance (Gulati and Nobile, 2016). To eradicate biofilms increased concentrations of antifungal drugs are required to treat an infection and if the administered dosage is below the minimum inhibitory concentrations (MIC), the chances of the pathogen to develop resistance increases.

The mechanisms of resistance include the development of efflux pumps that remove drugs from cells, changes to drug targets, an increase in enzymes that break down drugs and/or overproduction of the drug target to increase the minimum effective dose of the drug. In *C. albicans* biofilms, fluconazole resistance arose through the development of efflux pumps and reduction of the ergosterol content in the cell membranes (Mukherjee *et al.*, 2003).

Furthermore, microbes can transfer these resistance traits to other organisms. A study by Levy (2002) reported that individuals sharing the same environments, had microbes in their skin biomes that shared the same types of antibiotic resistance, showing that antibiotic resistance can be transferred simply by sharing the same living space. Another mechanism is the presence of persister cells that are metabolically inactive, reducing the uptake and effectiveness of most drugs. This gives rise to multidrug resistant (MDR) subpopulations (Figure 1.1) (LaFleur *et al.*, 2006).

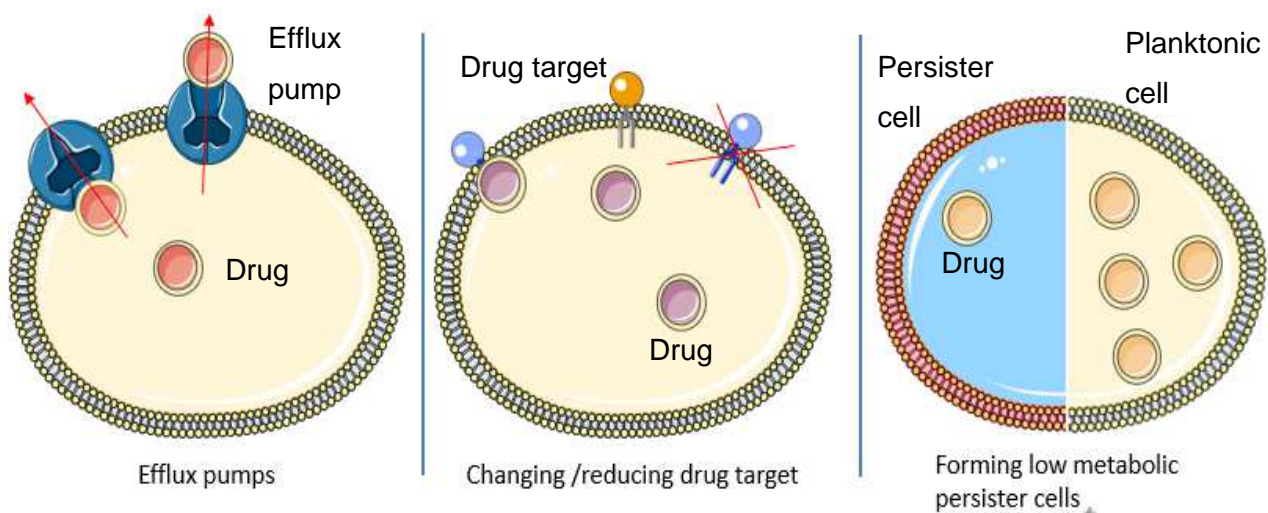


Figure 1.1: Three common mechanisms of resistance in *C. albicans*. (1) The production of efflux pumps removes the drug from the cell, thereby lowering the cellular concentrations of the drug. (2) By changing or reducing the number of certain targets or molecules. For example, a reduction of the amount of ergosterol in the cell membrane, reduces the effectiveness of drugs such as fluconazole. (3) In biofilms, the formation or presence of resistant, low metabolic persister cells can cause reoccurrence of the infection after drug treatment (LaFleur *et al.*, 2006).

Since microbes are developing resistance to antibiotics faster than new drugs can be developed, it is critical to find new ways to combat infectious diseases. Therefore, both novel drugs and treatment strategies are required to treat *C. albicans* infections and prevent MDR development. Antimicrobial peptides (AMPs) are a class of molecules that have antimicrobial, immunomodulatory and anti-biofilm activities. As such they are promising leads for the development of novel antifungal agents to treat *C. albicans* infections and prevent MDR development.

1.2 Antimicrobial peptides

1.2.1 Leads for novel antimicrobial agents

The first identified and studied AMPs were found in small invertebrates such as the silk moth and *Drosophila* fruit flies. These studies focused on how AMPs were induced by challenging the organism with bacteria and fungi (Zasloff, 2002). Most insects were found to have some form of AMP production as part of the innate immune system. AMPs were also identified as part of innate immunity in humans, and were identified to have multifunctional properties including the regulation of inflammation, chemotactic effects on immune cells and the signalling of infection in the body. Consequently, AMPs as multifunctional peptides not only directly disrupt microbial growth but also aid the host's immune system in the process (Hancock and Diamond, 2000).

Not only do a wide range of organisms produce AMPs, but there is a remarkable diversity in AMP structure regarding size, sequence, and charge. Yet, AMPs do share common characteristics which

are that most AMPs are amphipathic, have positive net charges at a physiological pH, and are between 10 and 50 amino acid residues in size (Chung and Khanum, 2017).

There are four general structural classifications of AMPs and these are α -helical, β -sheet, extended structures, and looped peptides (Figure 1.2)(Mojsoska and Jenssen, 2015). Peptides with β -sheets or α -helices are generally more common, although looped peptides and linear peptides with segregating hydrophilic and hydrophobic residues can also be found (Zaslhoff, 2002, Yeung *et al.*, 2011).

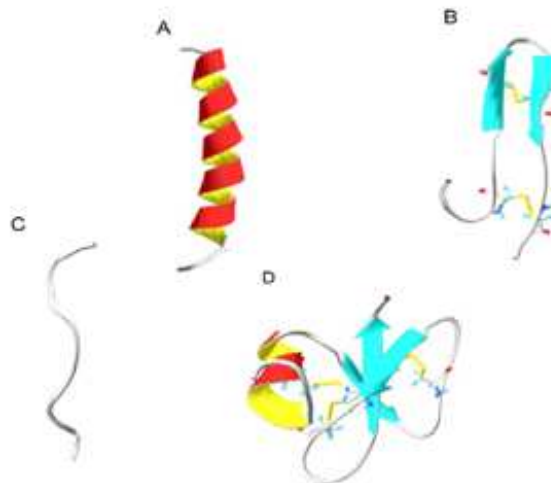


Figure 1.2: The four structural classifications of AMPs. (A) α -helical secondary structures are usually amphipathic with one side being hydrophobic and the other side being hydrophilic. (B) β -sheeted secondary structure usually facilitates the interaction between an AMP and the plasma membrane of cells. (C) Linear secondary structure. This class of AMPs usually do not have one fixed secondary structure but rather changes depending on the structure or molecule with which it interacts. (D) Looped secondary structure are usually cross-linked by disulphide bonds and these peptides are generally sensitive to reducing environments (By Biljana & Havard, 2015, used under CC-BY-NC 2.0 user license).

Many AMPs are effective against both bacterial and fungal cells due to their different cell specific modes of action (van der Kraan *et al.*, 2005). Antifungal peptides (AFP) are a sub-class of AMPs and the most common natural source of these peptides are plants, more specifically, the plant defensins (Yan *et al.*, 2015). Unlike other defensins which are usually more active against bacteria, plant defensins are generally more effective against a broad range of fungi. This is hypothesized to be due to the general threat that fungi pose to plants. Still, these defensins are active against non-phytopathogenic fungi, such as *C. albicans* (Stotz *et al.*, 2014).

Challenges associated with the development of AMPs including AFPs as therapeutic agents are related to selectivity and stability including the effects of salt and proteolytic enzymes. Fungi are eukaryotic and therefore membrane targeting may also adversely affect mammalian cells. Therefore, in fungi such as *C. albicans*, the ability of AFPs to target molecules such as ergosterol,

laminarin and mannan would result in selective targeting. Most AMPs in clinical trials and used clinically are administered as creams, gels, hydrogels or mouth washes (Table 1.1). These methods of application or administration are due to the salt and proteolytic sensitivity of AMPs. These effects can be overcome by developing analogues in which for example all D-amino acids instead of L-amino acids are used, to reduce the risk of protease digestion whilst retaining antimicrobial activity (Zasloff, 2002). Other compounds like ion chelators added to the peptide solutions reduce the concentration of free ions in environments with high salt concentrations. Nonetheless, the first step in identifying an AMP for further development is to determine the activity and mode of action before this peptide can be modified for evaluation in high salt and proteolytic environments.

Several AMPs have been developed and are in clinical trials or are used clinically. The phase of clinical trial, indication/s and manner of administration are summarised in Table 1.1.

Table 1.1: Reported peptides and peptidomimetics in commercial development. Since this record, some of these drug treatments have become available commercially. Adapted from Mahlapuu *et al.* (2016)

AMP	Description	Phase	Indication	Administration	Clinical trial identifier (if available)
Pexiganan (MSI-78)	Analog of magainin (skin of African clawed frog)	Phase III	Infected diabetic foot ulcers	Topical cream	NCT00563394, NCT00563433
Omiganan	Derived from indolicidin (bovine)	Phase II/III	Catheter infections and rosacea	Topical gel	NCT00231153, NCT01784133
Lytixar (LTX-109)	Synthetic antimicrobial peptidomimetic	Phase I/II	Uncomplicated Gram-positive skin infections, impetigo, and nasal colonization with <i>S. aureus</i>	Topical hydrogel	NCT01223222, NCT01803035, NCT01158235
hLF1-11	Derived from lactoferricin (human)	Phase I/II	Bacteraemia and fungal infections in immune-compromised haematopoietic stem cell transplant recipients	Intravenous treatment (in saline)	NCT00509938
Novexatin (NP-213)	Derived from defensins (human)	Phase II	Onychomycosis (fungal nail infection)	Topical brush-on-treatment	
CZEN- 002	Dimericoctamer derived from α -MSH(human)	Phase IIb	Vaginal candidiasis	Vaginal gel	
LL-37	LL-37 (human)	Phase I/II	Hard-to-heal venous leg ulcers	Polyvinyl alcohol-based solution	
PXL01	Derived from lactoferricin (human)	Phase II	Prevention of post-surgical adhesion formation in hand surgery	Hyaluronic acid-based hydrogel	NCT01022242
Iseganan (IB-367)	Derived from protegrin 1 (porcine leukocytes)	Phase III	Oral mucositis in patients receiving radiotherapy for head and neck malignancy	Oral solution	NCT00022373
PAC-113	Derived from histatin 3 (human saliva)	Phase II	Oral candidiasis in HIV seropositive patients	Mouth rinse	NCT00659971

1.2.2 Modes of action

Cell wall targets

One of the main targets for drug development is the cell wall of *C. albicans*. This structure consists mainly of polysaccharides, such as β -glucans and chitin, cross-linked by proteins (Figure 1.3) (Klis *et al.*, 2001). Since these structures and associated pathways of synthesis are not present in mammalian cells, they are good drug targets. Binding of a drug to the polysaccharides or proteins on the cell wall and membrane can cause destabilisation thereby compromising cellular function.

Several AMPs have the ability to bind to and disrupt fungal cell walls (Maurya *et al.*, 2011). In addition, binding may be an initial event required for the subsequent interaction with the cell membrane. For example, laminarin and mannan are common components of the cell wall of *C. albicans*. Laminarin is a glucan-polysaccharide that contains 1,3-linked β -D-glucose residues with 1,6-linked branches forming at a ratio of 1:3 (Salyers *et al.*, 1977). Mannan is a linear polymer of mannose with $\beta(1-4)$ linkages (Petersen *et al.*, 2001). Both polysaccharides are present on the cell surface strengthening the cell wall, promoting cellular adherence and communication (Chaffin, 2008). Disruption either by binding or the inhibition of cellular biosynthesis of these polysaccharides can compromise cellular function. Several proteins, including the insect β -Glucan recognition protein (β GRP), and AMPs recognize and bind to fungal cell wall components (Takahashi *et al.*, 2014).

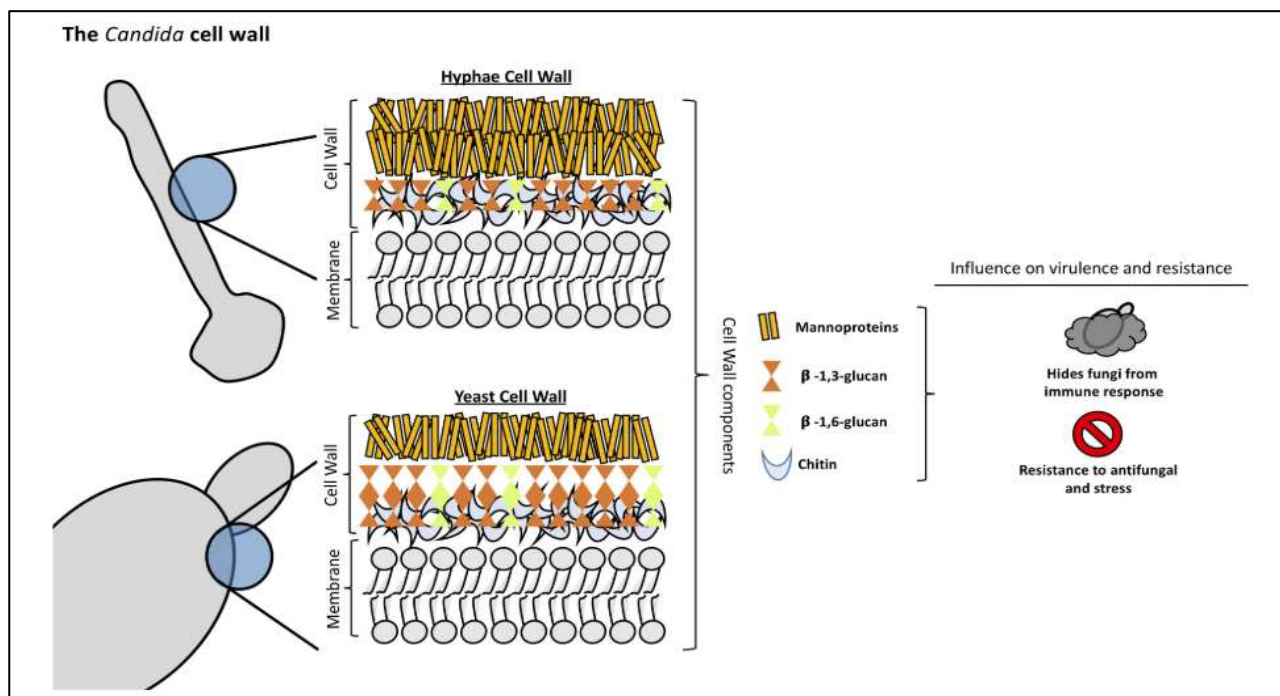


Figure 1.3: Simplified representation of the structure of the cell wall of *C. albicans*. Directly above the plasma membrane is the cell wall, mainly composed out of chitin and β -glucans, cross-linked by short protein sequences. Associated with the cell wall are different glycoproteins and polysaccharides, such as mannan and laminarin. This structure helps contribute to the virulence and resistance of the cell (Garcia-Rubio *et al.*, 2019).

Cell membrane acting

For most AMPs, their mode of action and antimicrobial effects are still unknown. One mode of action, widely studied, involves the permeabilization of the cell membrane (Brogden, 2005) and to date, there are three proposed mechanisms of AMP mediated cell membrane permeabilization (Figure 1.4).

The first is the barrel-stave model in which peptides associate with the cell membrane and self-aggregate to form barrel-like, aqueous pores in the membrane. The second model is the toroidal pore model, where the peptide associates with polar head groups of the cell membrane, causing the membrane to curve and self-associate between leaflets to form a pore within the membrane. Finally in the carpet model peptides line the membrane in a carpet-like manner and aggregate to break the membrane without hydrophobic interactions which form micelles in a detergent-like manner (Park *et al.*, 2011, Chung and Khanum, 2017).

Mechanisms of antimicrobial peptides on cell membranes

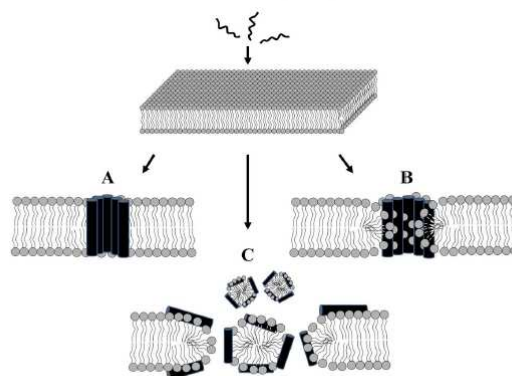


Figure 1.4: Different models for membrane permeabilization by antimicrobial peptides. (A) The barrel-stave model: peptides self-aggregate to form aqueous pores in the cell membrane. (B) The toroidal pore model: peptides associate with polar head groups of lipids and self-aggregate to curve the two lipid bilayers together. (C) The carpet model: peptides line the polar headgroups of lipids in a carpet-like manner to separate lipid interactions and form micelles in a detergent-like manner (Park *et al.*, 2011).

Membrane depolarization

Interaction of AMPs with the cell membrane can cause membrane depolarization. Normally there is an uneven distribution of metal cations inside and outside of the cell membrane creating an electrostatic potential gradient across the cell membrane (Arino *et al.*, 2010). This membrane potential is regulated by different membrane protein transporters, such as the $\text{Na}^+(\text{K}^+)/\text{H}^+$ antiporters and the $\text{Na}^+(\text{K}^+)\text{-ATPase}$ transporters (Arino *et al.*, 2010). When this membrane potential becomes disrupted it can have detrimental cellular effects that include the build-up of toxic amounts of intracellular sodium and the disturbance of processes that rely on the membrane potential e.g. glucose uptake (Ramos *et al.*, 2011)(Figure 1.5).

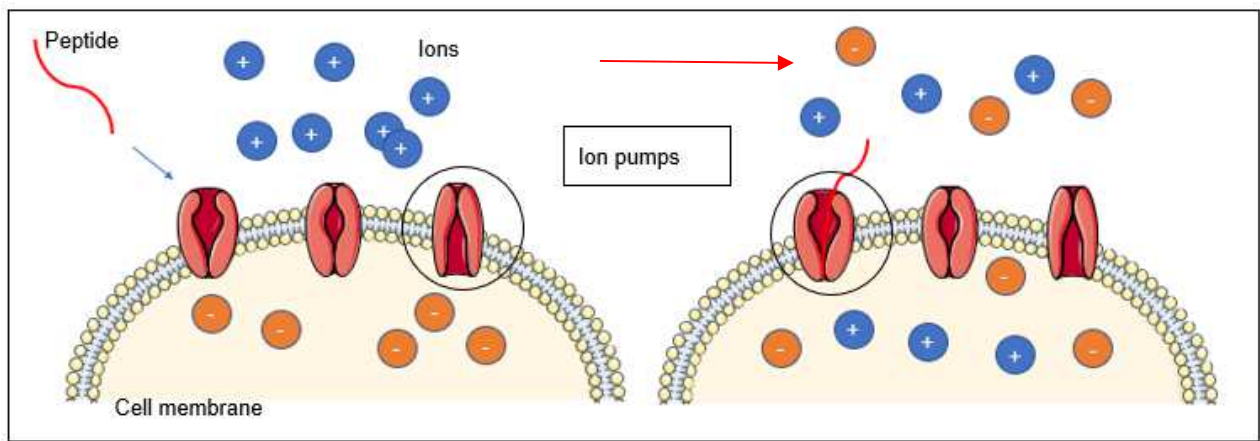


Figure 1.5: A representation of a cell membrane containing membrane proteins responsible for maintaining an electrostatic potential across the membrane. The model peptide interferes with membrane protein (Na⁺/K⁺-pumps, Cl⁻-channels etc.) function, causing depolarization of the membrane. If the peptide would disrupt the membrane potential by damaging the cell membrane, this could be considered membrane permeabilization rather than membrane depolarization.

Antifungal drugs, such as fluconazole, are known to affect the membrane potential of *C. albicans* (Elicharova and Sychrova, 2013). In addition to this, some peptides have also shown the ability to cause membrane depolarization in *C. albicans*. APP is a 20-amino acid peptide derivative (GLARALTRLLRQLTRQLTRA) of the cell penetrating peptide ppGT20, which was originally designed for single-gene transfer across cell membranes (Rittner *et al.*, 2002). This peptide was shown to cause potassium efflux and nucleotide leakage in *C. albicans* (Li *et al.*, 2016), identifying membrane proteins responsible for maintaining the membrane potential as possible targets for drug treatment. Likewise the peptide K19Hc caused membrane depolarization and permeabilization (Jang *et al.* (2006).

Vacuoles and other intracellular targets

Recent research has shown that many AMPs have intracellular targets including DNA, RNA and organelles such as the mitochondria and vacuoles (Maurya *et al.*, 2011). By better understanding the structure and the function of organelles like these, better therapies and drug treatments can be developed.

The vacuoles located in the cytosol are important intracellular structures and targets of some AMPs (Figure 1.6). A few of the functions of vacuoles include receiving nutrients and other molecules taken up through endocytosis, aiding in protein sorting during cell growth and supplying nutrients to budding daughter cells. This acidic organelle is similar to the lysosome found in mammalian cells. Vacuoles play an important role in stress responses, adaptation to different environments and cell differentiation (Rane *et al.*, 2013). Studies have shown that vacuoles are important to the virulence and pathogenesis of *C. albicans* (Johnston *et al.*, 2009, Palmer *et al.*, 2003, Palmer, 2011, Veses *et al.*, 2008). Vacuole membrane components such as transport proteins signal to the cell to respond

to environmental changes. In addition, the vacuoles remove harmful molecules from the cytoplasm (Veses *et al.*, 2008).

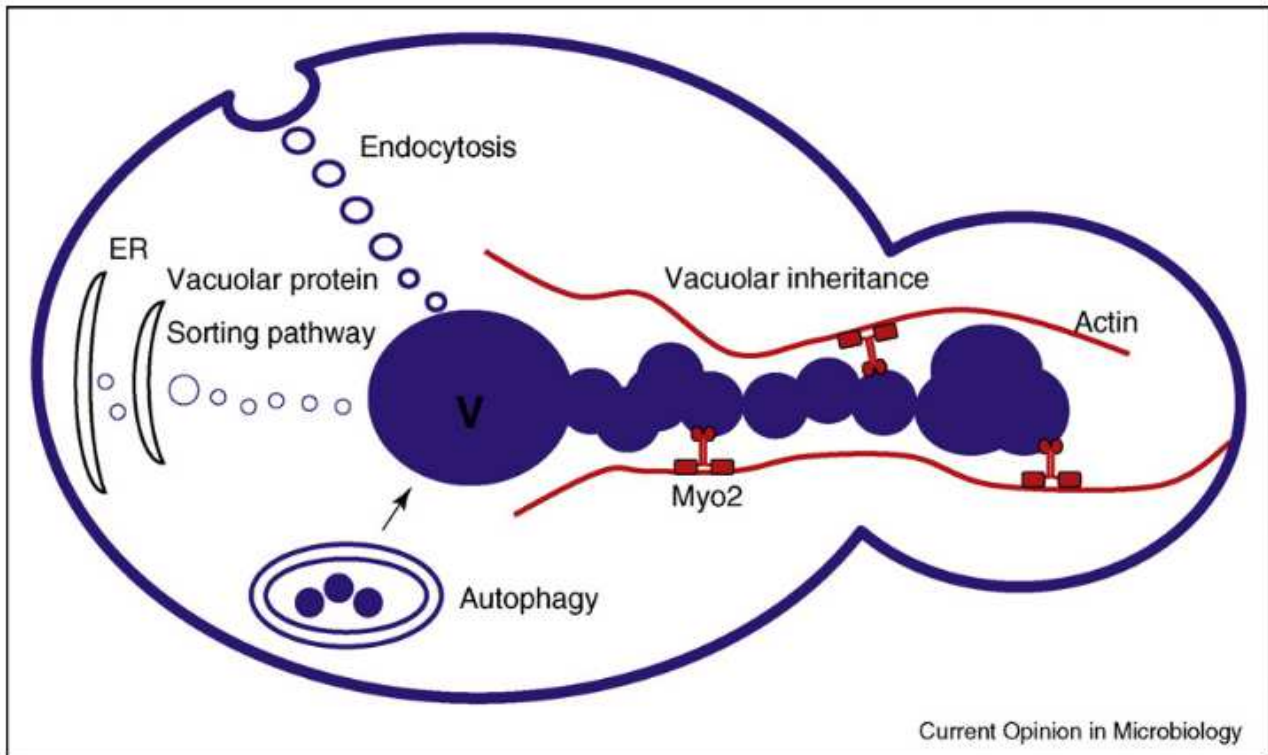


Figure 1.6: Convergent membrane trafficking involving the pathways for vacuole protein sorting, endocytosis, autophagy and vacuole inheritance in budding yeast. A stream of vacuole vesicles that form the vacuole segregation structure, which is mobilised by the Myo2-actin cytoskeleton is also shown (Veses *et al.*, 2008).

pVEC, a cell penetrating peptide with activity against *Candida* species, has been shown to target vacuoles and other organelles (Gong and Karlsson, 2017). The authors investigated localisation of pVEC using 5-FAM-pVEC and stained vacuoles using CellTracker-Blue(CMAC) (CTB-CMAC)(Figure 1.7). At low concentrations there was an equal distribution of 5-FAM-pVEC and vacuole staining, while at high concentrations, only 5-FAM-pVEC staining was observed, indicating that in a dosage dependent manner pVEC targeted the vacuoles. Whether the observed effect was due to direct vacuole membrane targeting or disruption of vacuole related processes was not determined.

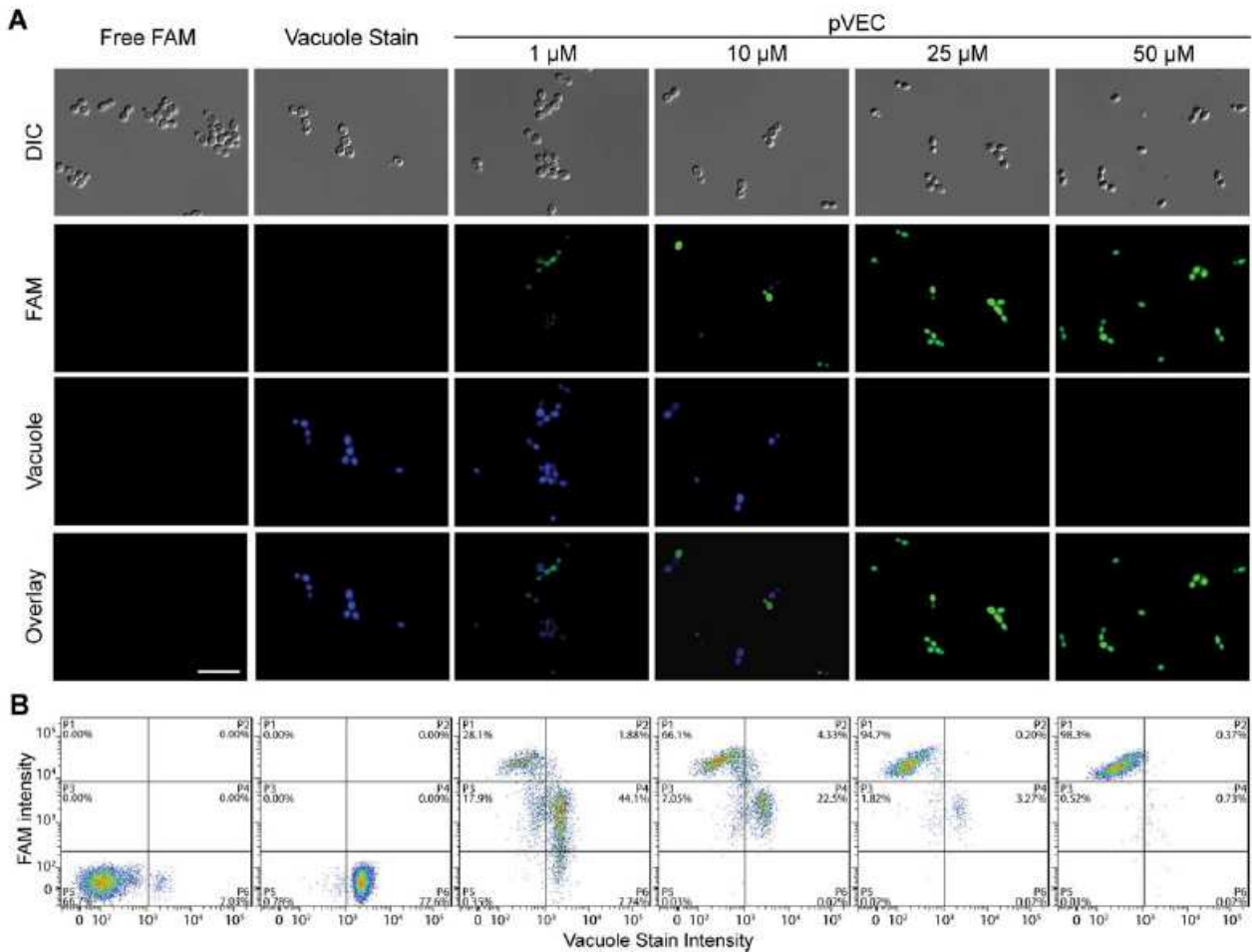


Figure 1.7: Intracellular distribution of pVEC in *C. albicans* at different peptide concentrations. (A) Differential interference Contrast (DIC) and fluorescence microscopy images showing location of FAM-labelled pVEC and location of vacuoles, stained with CellTracker-Blue (CMAC) in cells. (B) Flow cytometry data illustrating shift of FAM and vacuolar fluorescence. For (A), scale bar=510 mm. Results published by Gong and Karlsson (2017).

1.3 Methods for determining the mechanisms of action of AMPs

Over the past two decades, a wide variety of methods have been developed and optimized to determine the different modes of action of AMPs. These methods range from using light microscopy and electron microscopy to using flow cytometry and different molecular markers. Most studies aimed at determining the modes of action of a peptide start by looking at the outside of the cell and moving inwards. This means that the effects of the peptide on the membrane and cell wall are studied first. This is usually done with the use of electron microscopy and fluorescent microscopy. By looking at differences in cell structures of treated and untreated cells with the use of scanning electron microscopy (SEM) and transmission electron microscopy (TEM), researchers were able to investigate how the peptide interacts with the membrane of a target cell. An example of this was a study done by Taute (2017) where the effects of the peptides Os and Os-C on bacterial cell walls and cell membranes were observed using SEM.

Researchers have also investigated whether peptides bind to certain components of the fungal cell wall (Jang *et al.*, 2006). This was done by adding laminarin or mannan, two important components of the fungal cell wall, to peptide solutions before treating cells. Decreased activity indicated that the peptides interacted with free laminarin or mannan, inhibiting activity on the cells. This showed that the peptide does not just affect the cell membrane in a random fashion similar to detergents, but in fact interacts with cell wall components as well, interfering with its structure and stability. In order to obtain more detailed information on the binding of a peptide, further experiments are required. One such method is known as Isothermal titration calorimetry (ITC). This method is used to determine the different parameters and binding kinetics of a molecular interaction by measuring the change in temperature when different concentrations of two molecules are mixed together (Freire *et al.*, 1990).

Peptides are known to destabilize or depolarize cell membranes. This has previously been tested by measuring parameters such as potassium efflux rates of cells (Orlov *et al.*, 2002). A study done by Jang *et al.* (2006) tested the effects of a peptide K19Hc on potassium efflux of treated *C. albicans* cells. The amount of potassium in the surrounding medium after cells were treated with the peptide was measured using an Ion selective electrode (ISE) meter fitted with a potassium ion electrode. High amounts of released potassium indicated cell permeabilization and membrane depolarization.

When looking deeper into cells, methods such as flow cytometry and fluorescent microscopy, are used to determine how peptides affect intracellular targets such as vacuoles and mitochondria. Some studies have even shown peptides that interact with DNA molecules (Feng *et al.*, 1997). Taute *et al.* (2015) previously showed that Os interacts with plasmid DNA by using gel electrophoresis and studying DNA migration retardation of plasmids exposed to Os.

1.4 Background to the study

Defensins are a family of cationic peptides with an average length of 29 to 34 amino acids. The class was first identified in rabbit and guinea-pig neutrophils (Zeya and Spitznagel, 1963) and later in other vertebrates as well as invertebrates and plants. Most peptides in this class are rich in arginine residues and contain multiple cysteine residues that lead to disulphide bonds (Ganz *et al.*, 1990). Defensins are responsible for the innate immunity in organisms such as plants and insects but can have additional effects in mammals, such as the chemotaxis of leukocytes (Wong *et al.*, 2007). The general mode of action of defensins, whether from vertebrate, invertebrate or plant cells, is the disruption of microbial cell membranes. Research has identified a range of intracellular targets in addition to targeting and disrupting cellular membranes:

The first reported tick defensin was a partial amino acid sequence purified from the haemolymph of *Ornithodoros moubata* (Van der Goes van Naters-Yasui, 2000). It was later discovered that four different defensins are secreted into the midgut of the tick after blood feeding to serve as a first line

of defence against infection (Nakajima *et al.*, 2003). Since then a range of different defensins have been discovered in ticks, including OsDef2 identified in *O. savignii* (Prinsloo *et al.*, 2013). The majority of defensins identified in ticks do not significantly differ from those found in insects and usually have 6 cysteine residues forming disulphide bonds, and are positively charged with affinity for the major phospholipids in bacterial cell membranes (Gillespie and *et al.*, 1997). The defensins from hard and soft ticks differ slightly and generally protect ticks from bacterial and fungal infections (Taylor, 2006). Tick defensins have some unique characteristics and sequences that could make them good candidates to be developed as AFPs for the treatment of fungal infections.

The peptide Os, investigated in this study, is the carboxy-terminal derivative of the defensin protein OsDef2 identified in the tick *O. savignii* (Prinsloo *et al.*, 2013). The sequences of the parent peptide OsDef2 and the derivative Os are shown in Table 1.2. A summary of the effects and known modes of action of Os is presented in Table 1.3.

Table 1.2: The original peptide and the Os derivative along with their sequences, lengths, mass and charge at physiological pH.

Peptide	Sequence	Length	Mass (Da)	Charge (pH 7.4)
OsDef2	GYGCPFNQYQCHSHCKGIRGYKGGYCKGAFKQTCKCY	37	4185.80	+6
Os	KGIRGYKGGYCKGAFKQTCKCY	22	2459.92	+6

Initial studies showed that the OsDef2 peptide was mainly effective against Gram-positive bacteria. The derivative Os was found to rapidly kill both *Escherichia coli* and *Bacillus subtilis* using antibacterial assays. *In vitro* studies showed that Os was not toxic towards mammalian cells and displayed antioxidant activity (Prinsloo *et al.*, 2013, Taute *et al.*, 2015). Ultrastructural studies indicated that Os caused bacterial cell wall indentation and the collapse of cellular structures and was able to permeabilize bacterial cell walls without causing cell lysis (Taute, 2017). In addition, Os was found to bind to plasmid DNA (Taute, 2017).

Table 1.3: Properties of Os identified in previous studies.

Property	Description	Publication
Antibacterial activity	Activity against Gram-positive and -negative bacteria.	Taute (2017), Prinsloo <i>et al.</i> (2013)
Known cellular targets		
Induction of reactive oxygen species (ROS)	Causes an increase in ROS in planktonic <i>C. albicans</i> but does not correlate with killing.	Unpublished results
Intracellular targets	Binds to plasmid DNA.	Taute (2017)
Membrane activity	Membrane permeabilization in bacteria, fungi and synthetic liposomes.	Taute (2017), (Ismail <i>et al.</i> , 2019), Unpublished results
Active transport across plasma membrane	Uptake into <i>C. albicans</i> cells significantly reduced in cells deprived of adenine-triphosphate.	Unpublished results
Advantages		
Cytotoxicity	No cytotoxicity in human erythrocytes, L929 fibroblasts or RAW 264.7 cells.	Taute (2017), Malan <i>et al.</i> (2016)
Antioxidant	Reduces the amount of ROS in solution and cellular models.	Prinsloo <i>et al.</i> (2013), Taute <i>et al.</i> (2015)
Structure	Circular dichroism showed an α -helical structure in a membrane-mimicking environment.	Prinsloo <i>et al.</i> (2013), Taute (2017)
Challenges		
Salt sensitivity	Loses activity (including antiplanktonic activity against <i>C. albicans</i>) in complex media and solutions with high salt concentrations.	Mbuayama (2016)
Cell wall interaction	Loses activity in the presence of high concentrations of polysaccharides found in fungal cell walls, such as mannan and laminarin evaluated with radial diffusion assay (RDA).	Unpublished results

Structural predictions using the sequence of the peptide and circular dichroism showed that Os most likely takes on an α -helical conformation when interacting with liposomal structures, such as cell membranes (Prinsloo *et al.*, 2013). Os has a positive net charge of +6, which allows it to electrostatically interact with negative polar head groups of lipids in bacterial and fungal cell membranes. The peptide is also amphipathic, which allows it to insert into lipid bilayers and disrupt membrane structures.

Os has antifungal activity with a minimum fungicidal concentration (MFC) of 6 μ M against planktonic cells (Mbuayama, 2016) when evaluated with the radial diffusion assay (RDA). However, activity against planktonic cells was lost in complex media such as Roswell Park Memorial Institute medium

(RPMI), possibly due to the high content of salts in complex media. Further unpublished findings showed that Os loses activity when pre-incubated with excess free laminarin or mannan which suggests that binding is essential for antifungal activity. To better understand this interaction, more in-depth analytical studies are required. Indications are that Os is cell membrane acting as it causes the permeabilization of liposome (*Saccharomyces cerevisiae* polar extract and 30% ergosterol) membranes with a 50% permeabilization concentration of 4 μ M. Therefore, the cell membrane and membranous organelles such as the vacuoles in fungi are potential targets.

1.5 Aim of the study

The main aim of this study was to further investigate the mode of action of the antimicrobial peptide Os in planktonic *Candida albicans* ATCC 90028 cells.

1.5.1 Objectives

1. To determine the concentration inhibiting 50% cell growth (IC_{50}) of Os with a modified micro-broth dilution assay.
2. To evaluate the effects of Os on cell wall morphology and intracellular structure of planktonic *C. albicans* cells using SEM and TEM, respectively.
3. To investigate the binding kinetics of Os to mannan and laminarin, major polysaccharides in the cell wall of *C. albicans*, using ITC and the modified microbroth dilution assay.
4. To study whether Os causes membrane depolarization of planktonic *C. albicans* cells.
5. To determine whether FAM labelled Os interacts with or targets vacuoles using flow cytometry and confocal laser scanning microscopy (CLSM).

2 Methodology

2.1 Overview

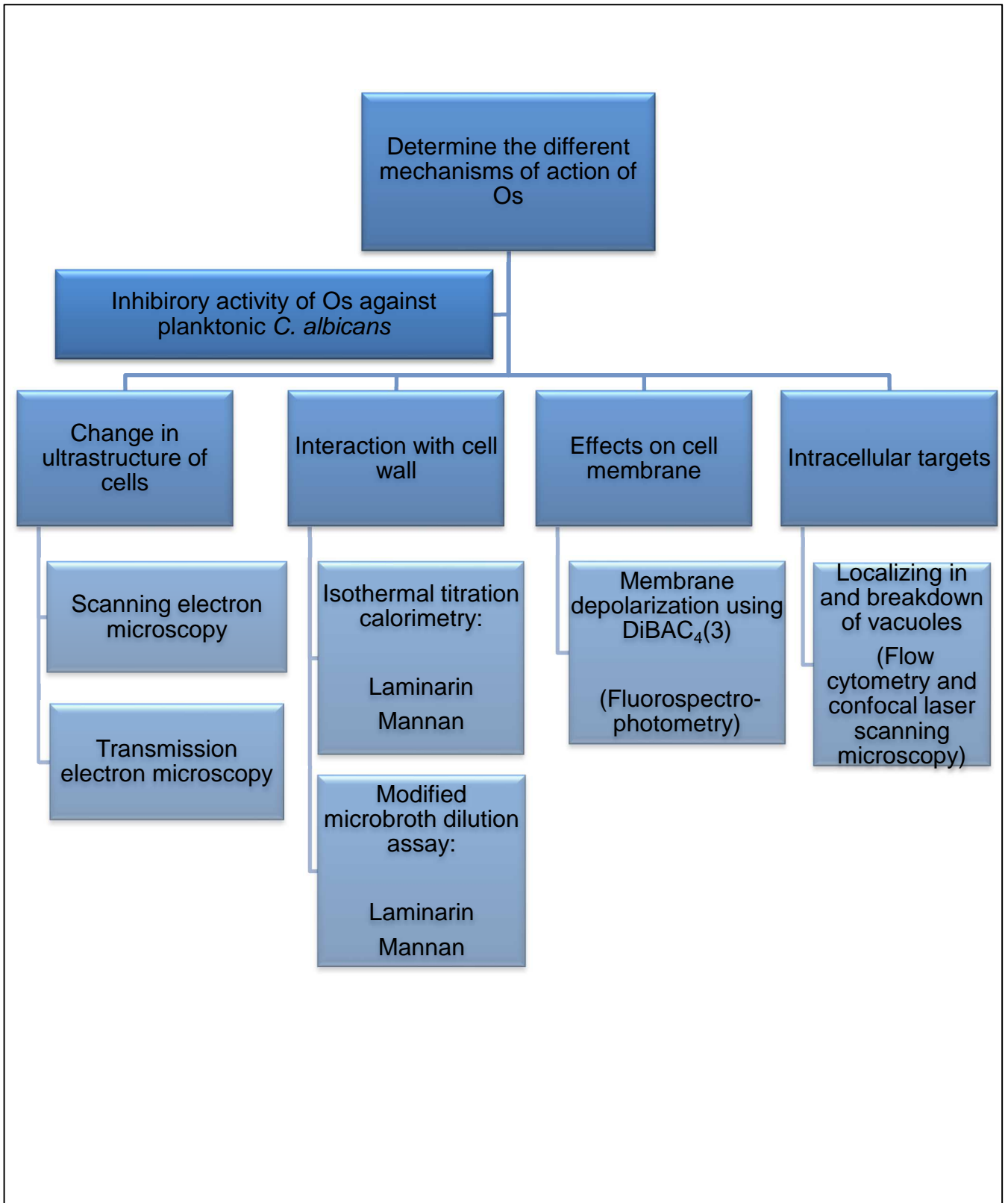


Figure 2.1: An overview of the methodology and the different techniques used in the study.

2.2 Chemical reagents

RPMI and yeast peptone dextrose (YPD) agar used for the cultivation of *C. albicans* was obtained from Sigma Aldrich, USA. Glucose supplementing RPMI in microbroth assays was obtained from Merck, RSA. 3-(*N*-morpholino) propanesulfonic acid (MOPS) buffering the RPMI medium was obtained from Sigma Aldrich, Johannesburg, RSA. CellTiter Blue (CTB) used to test cell viability in microbroth dilution assays was obtained from Anatech, Randburg, RSA. Amphotericin B (AmpB), a positive control was obtained from Sigma Aldrich, SA. *C. albicans* (ATCC90028) glycerol stocks were used for all experiments. Reagents for the preparation of sodium phosphate (NaP) buffer and other solutions was obtained from Merck, RSA. Poly-L-lysine for glass coverslips was obtained from Sigma Aldrich, Johannesburg, RSA. Laminarin and mannan used for cell wall binding assays were obtained from Sigma Aldrich, Johannesburg, RSA. DiBAC₄(3), fluorescent dye in membrane depolarization assays, was obtained from Molecular Probes, ThermoFisher Scientific, Johannesburg, RSA. CellTracker Blue-CMAC was also obtained from ThermoFisher Scientific, Johannesburg, RSA.

2.3 Synthesis of peptides and preparation of peptide solutions

Os and 5-FAM labelled Os was synthesized using FlexPeptide™ by GenScript (New Jersey, USA). The purity and molecular masses of the peptides were determined using reversed-phase high-performance liquid chromatography and mass spectroscopy, respectively. Melittin and 5-FAM labelled penetratin were also obtained from GenScript (New Jersey, USA). The lyophilized peptides may contain between 10 – 70% of bound salts and water by weight, therefore the concentration of the stock peptide solutions were determined using the molar extinction coefficients of Tyr (1200 Au/mmol/mL) and Trp (5560 Au/mmol/mL) and the following equation:

$$c = \frac{A \times d \times MW}{n(\epsilon_{Tyr}) + n(\epsilon_{Trp})}$$

where *c* is the concentration (mg/mL), *A* is the absorbance at 280 nm, *n* is the number of Tyr or Trp residues of each respective peptide and ϵ_{Tyr} and ϵ_{Trp} are the extinction coefficients of Tyr and Trp, respectively. Stock solutions of 160 μ M were prepared in filtered, double distilled water (ddH₂O) and stored at -20 °C.

2.4 Anti-planktonic microbroth dilution assay

The antifungal activity of Os against planktonic *C. albicans* cells was previously determined with the RDA and the spread plate method (Mbuayama, 2016). Both assays are time consuming and require several resources, often taking two to three days to obtain results from a single experiment. Researchers developed the microbroth dilution assay for the cost-effective and rapid determination

of the antimicrobial activity of drugs including AMPs. However, due to the salt sensitivity of Os (Table 1.3) standard microbroth dilution assays cannot be used. To overcome this limitation the modified microbroth dilution assay was developed to determine the IC₅₀ of Os and to further investigate its mode of action.

Firstly, the minimum percentage dilution of RPMI required for the optimal growth of *C. albicans* was determined. Secondly, in a reduced nutrient environment cells become more sensitive to the effects of drugs, therefore the activity of AmpB (positive control; not salt sensitive) in a reduced media environment was determined with the modified microbroth dilution assay.

To optimize growth conditions, *C. albicans* cells from frozen glycerol stocks were streaked over YPD agar plates and incubated at 37°C (Separation Scientific, Cape Town, RSA) for 24 hours. An overnight culture was prepared from the streak plate by picking 4-5 colonies and inoculating 20 mL of YPD broth. The culture was grown for 16 hours at 30°C with shaking at 150 rpm. Then, 100 µL of the culture was transferred to 9900 µL of fresh YPD broth. The subculture was incubated for 3 hours at 30°C with shaking until the culture reached an optical density (OD) of 0.50 at 620 nm measured with a UV-1600 PC VWR spectrophotometer (Separation Scientific, PA, USA).

Previous experiments showed that at an OD of 0.50 was equivalent to a cell concentration of 10⁶ cfu/mL. After incubation 7x 1 mL aliquots of culture were centrifuged for 10 min at 2300 x g (miniSpin Plus, Eppendorf, Merck). The supernatants were removed, and each cell pellet was washed with a range of RPMI dilutions (2%, 10%, 20%, 50%, 100%, 150% and 200%) with NaP buffer (pH 7.4, 20 mM) as diluent. All cells were collected by centrifugation at 14100 x g for 2 min. The supernatants were removed, and pellets were resuspended in the respective RPMI dilutions before being further diluted 5 times in the respective dilutions of RPMI. A 50 µL volume of the diluted cell suspensions were transferred to 6 wells for each dilution to polypropylene 96-well plates (Greiner Bio-One, Kremsmunster, Austria). To three wells of each RPMI dilution, 50 µL of AmpB (10 µM final concentration) was added. To ensure that RPMI did not interfere with quantification, triplicate blanks were included for each RPMI dilution and consisted of 50 µL RPMI dilution and 50 µL of ddH₂O. Cells were incubated at 37°C for 2 hours and cell viability was determined as described in section 2.4.1.

As shown in section 3.1, after 3 hours there were no significant differences in growth of planktonic *C. albicans* for 100% RPMI compared with medium or 10% RPMI diluted in NaP buffer (10 mM, pH 7.4) (10%RPMI/NaP). Therefore, 10%RPMI/NaP was used throughout this study in the modified version of the microbroth dilution assay.

To evaluate the drug sensitivity, of cell growth in RPMI media, cells were prepared as described earlier in 10%RPMI/NaP and were exposed to serial dilutions of the positive control, AmpB and Os

at final concentrations of 0.03 μM - 5 μM and 0.15 μM - 20 μM respectively for 2 hours at 37°C before the cell viability was determined and calculated as described in Section 2.4.1.

2.4.1 Cell viability

Cell viability was analysed using CTB. This fluorescent dye consists mainly of resazurin which is reduced by metabolically active cells to resorufin which is quantified with fluorescent spectrophotometry at an excitation wavelength (Ex) of 535 nm and an emission wavelength (Em) of 590 nm.

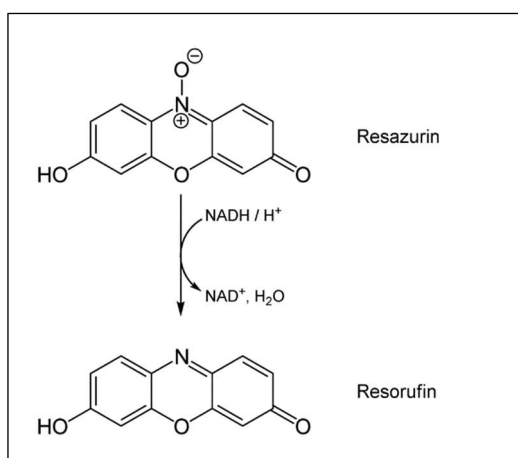


Figure 2.2: The chemical structure of resazurin, the chemical used in CellTiter Blue staining. In this assay, resazurin is reduced to resorufin, a fluorescent molecule, that is quantified as a measure of cell viability (ThermoFisher Scientific).

The method that was used is described by Troskie *et al.* (2014). After 2 hours of exposure, 11 μL of CTB was added to each well and after a further 1 hour incubation at 37°C, with a total exposure time of 3 hours, fluorescence was measured at an Ex of 535 nm and an Em of 590 nm (Spectramax, Multi-mode detection platform, Molecular Devices, Austria). The percentage inhibition was calculated using the following equation:

$$\text{Inhibition (\%)} = 100 - \frac{100 \times (\text{Avg. absorption} - \text{Avg. blank})}{\text{Avg. absorption of growth control} - \text{Avg. blank}}$$

From the generated curves the IC₂₅, IC₅₀ and IC₇₅ values were calculated and represent the concentrations of Os needed to inhibit 25%, 50% and 75% of cell growth respectively. In further experiments the mode of action of Os, the IC₂₅, IC₅₀ and IC₇₅ concentrations were used.

2.5 Coated glass coverslip preparation

For SEM and confocal microscopy, cells were mounted on 10 mm diameter glass coverslips (Lasec, Johannesburg, RSA). The coverslips were coated with positively charged poly-L-lysine which improves the attachment of negatively charged cells through electrostatic interactions with negatively charged polar head groups of plasma membrane lipids (Fischer *et al.*, 2008). Coverslips were washed with 10% NaOH (w/v), 60% ethanol (v/v) by shaking for 2 hours. The coverslips were rinsed with ddH₂O and sterilized with 99.9% ethanol (v/v). The coverslips were dried and submerged into poly-L-lysine solution (7000 – 15000 kDa, Sigma-Aldrich, Johannesburg, RSA) for 2 hours. Finally, the coverslips were rinsed three times with ddH₂O and were left to dry in a sterile environment for at least 3 days before use.

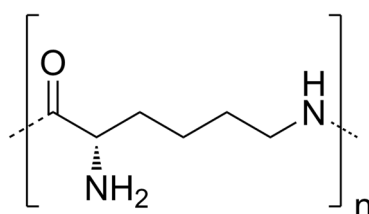


Figure 2.3: Chemical structure of the monomer unit of poly-L-lysine. Drawn using ChemSketch.

2.6 Scanning electron microscopy

The effects of AmpB and Os on the cell wall morphology of planktonic *C. albicans* cells was determined with SEM. This technique allows the high-resolution visualization of surface detail. Briefly, in SEM the sample is bombarded with electrons released from a tungsten filament. Areas of the sample with low conductivity can become charged with electrons, causing distortions in the final image. To eliminate this effect the sample is thinly coated with a layer of conducting material, such as gold or graphite, and lower energy electron beams in the range of 10 - 20 keV are used. A detector, in the form of a cathode-ray tube, picks up secondary electrons and backscattered electrons from the sample (Reimer, 2013) and this data is converted into an image with the use of software (Figure 2.3) (Bozzola and Russell, 1999).

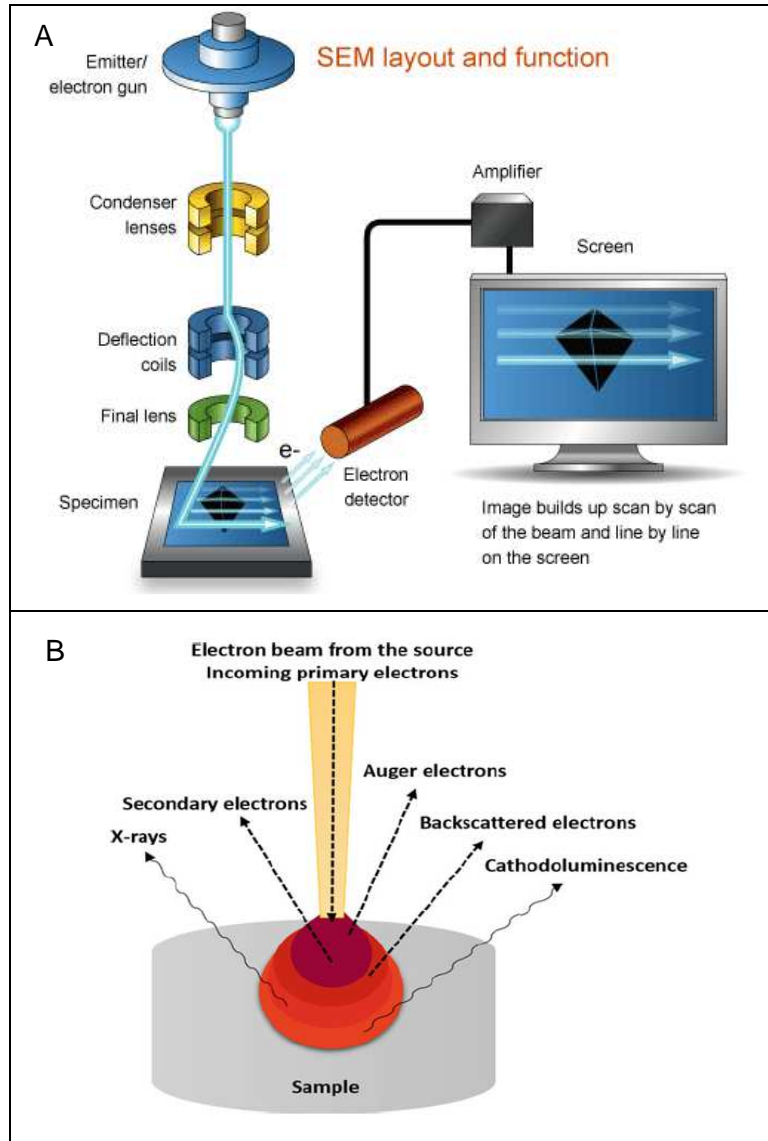


Figure 2.4: (A) The different components and layout of a scanning electron microscope. Accelerated electrons move through magnetic coils that function in the same way glass lenses do in light microscopes. This guides the electron beam across the sample. Reflected electrons are captured by the electron detector and an image is generated with software based on the captured electrons (Kanakamedala, 2019). (B) Different interactions between electron beam and the sample. Secondary electrons are the main sources of information on the topology of the sample. Backscattered electrons are secondary sources of information about the textures and surfaces of the sample (Akhtar *et al.*, 2018).

The method that was used to treat and prepare cells for SEM analysis as described by Taute (2017) with modifications. Cells used in this experiment were prepared as described in section 2.4.1 and were exposed to the IC₂₅, IC₅₀ and the IC₇₅ of AmpB and Os for 3 hours. The *C. albicans* cells were fixed by adding 50 µL of 5% formaldehyde/glutaraldehyde solution, diluted with 75 mM NaP (pH 7.4), to each well of a 96-well plate. After fixation at room temperature for 15 minutes the cells were transferred to glass cover slips, coated with poly-L-lysine (Section 2.5) in 24-well plates (Greiner Bio-

One, Kremsmunster, Austria). Cells still in fixative were allowed to adhere at room temperature for 70 min. The cover slips were then washed three times with 75 mM NaP (pH 7.4) to remove non-adhered cells and fixative. Post-fixing was achieved with 1% OsO₄ for 45 min and then the excess OsO₄ was removed and the coverslips were washed three times with 75 mM NaP (pH 7.4). Samples were dehydrated with increasing concentrations of ethanol (30%, 50%, 70%, 90%, 100% v/v in ddH₂O), with three washes using 100% ethanol. After the final 100% ethanol wash, the ethanol was removed, hexamethyldisilazane (HMDS) was added for 1 hour. Afterwards, the HMDS was removed and 2 drops of HMDS was added to each coverslip. Coverslips were dried overnight before mounting onto aluminium stubs and coating with carbon. Coated samples were visualised using SEM (Ultra plus field emission gun, Zeiss, Oberkochen, Germany).

2.7 Transmission electron microscopy

With TEM, the effects of AmpB and Os on the cell wall, organelles and membranes were evaluated. TEM detects transmitted or scattered electrons, emitted by tungsten filaments that have interacted with cellular structures. The electron-intensity distribution between the sample and electron beam is focused by a series of magnetic lenses onto a fluorescent screen. In order to detect electrons that have interacted with the sample accurately, the sample has to be thin, between 5 nm and 500 nm. Additionally, due to the low electron-dense properties of biological samples (Reimer, 2013), biological material is stained with electron-dense metals, such as lead. This allows electrons to better interact with the typically low electron-dense biological sample and also provides slightly higher magnification and resolution (Figure 2.4) (Bozzola and Russell, 1999). Treated *C. albicans* cells was prepared for TEM as described by Park et al. (2006) with modifications.

Transmission electron microscope

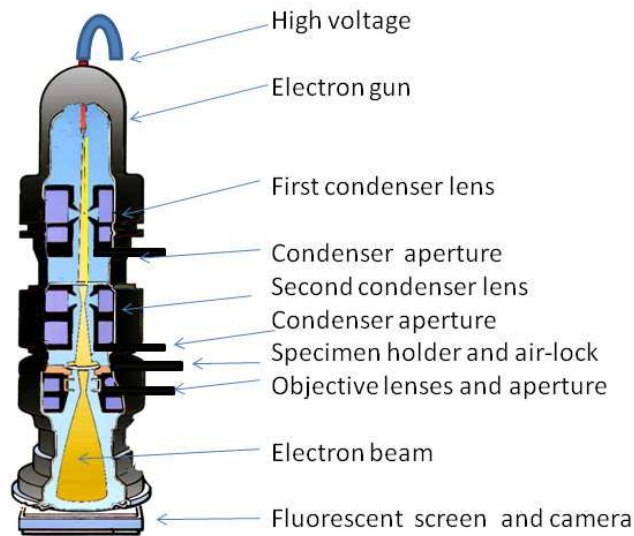


Figure 2.5: A diagram depicting the different components of a transmission electron microscope and showing how the electron beam is directed to interact with the tissue and to create an image (Beards, 2020).

Cells were treated in 0.6 mL Eppendorf tubes as described in section 2.4. After treatment, cells were centrifuged at 5000 x g for 10 min, washed with NaP buffer (75 mM, pH 7.4) before being fixed with formaldehyde/glutaraldehyde (2.5% v/v) in NaP buffer (75 mM, pH 7.4) for 1 hour at room temperature. After fixing, the cells were collected by centrifugation for 2 min at 2500 x g. The supernatants were discarded, and cell pellets were washed three times with NaP buffer (75 mM, pH 7.4) with centrifugation (2 min, 2500 x g) steps between each wash step. Post-fixing was undertaken using 300 μ L of 1% OsO₄ for 1 hour. This was followed by three more washes with NaP buffer. Cells were dehydrated with increasing concentrations of ethanol (30%, 50%, 70%, 90% v/v in ddH₂O) with three final washes of 100% ethanol. Cells were collected by centrifugation (2 min, 2500 x g) between each dehydration step. The final dehydration step was overnight in 100% ethanol. The 100% ethanol was removed and replaced with 50% Embed812 resin mixed with 100% ethanol (1:1 v/v). After an incubation time of 1 hour, the cells were collected by centrifugation and the supernatant was replaced with 100% Embed812 resin. After mixing for 4 hours, the samples were centrifuged again and new 100% Embed812 resin was added. The cell pellets were transferred to moulds and new resin was added. The samples were placed at 60°C for 48 hours to allow polymerisation of the resin. After polymerisation, the samples were trimmed and sectioned using a Leica Ultramicrotome (Leica Microsystems GmbH, Wezlar, Germany) and a 45° diamond knife (Diatome, Pennsylvania, USA). Sections were contrasted using uranyl acetate and lead citrate and left to dry overnight before being visualized using a JEM-2100 transmission electron microscope (JEOL, Tokyo, Japan).

2.8 Isothermal titration calorimetry

The interaction of Os with laminarin and mannan, components of the cell wall of *C. albicans*, was investigated using ITC. In ITC the binding kinetics is determined by measuring the change in temperature when solutions of the target molecules are mixed together. This change in temperature can be used to calculate the binding kinetics of two molecules using the equation for Gibbs free energy ($\Delta G = \Delta H - T\Delta S$) (Freire *et al.*, 1990). In addition to that, the change in temperature can also be used to determine the binding affinity of association constant (K_a) between two molecules.

In this experiment the binding affinity of the peptide to laminarin and mannan, two abundant polysaccharides in the cell wall of *C. albicans* (Figure 2.4) (Ruiz-Herrera *et al.*, 2006), was determined. Furthermore, unpublished results have shown that in a biological environment using the RDA, Os loses activity when incubated with an excess of laminarin or mannan. The purpose of using ITC was to obtain a better understanding of the interaction of Os with the identified polysaccharides.

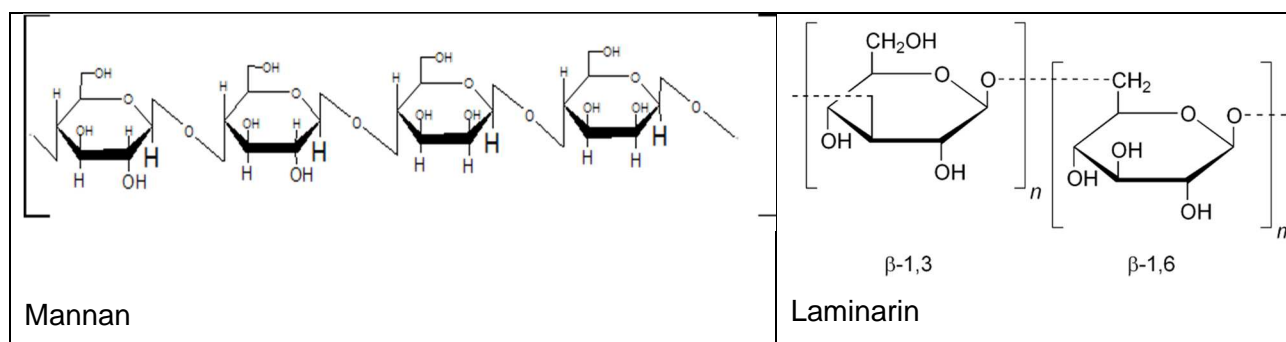


Figure 2.6: Chemical structures of cell wall components, mannan (left) and laminarin (right) found in *C. albicans* cell walls. Drawn using ChemsSketch.

The experimental design was as described by Nevidalova *et al.* (2018) with some modifications, and concentrations used were based on the method of Mishima *et al.* (2009). For ITC the MicroCal₂₀₀ (Malvern Panalytical, Malvern, USA) was used. Briefly, Os was present in the sample cell, with mannan or laminarin present in the syringe. Different concentrations of Os and laminarin/mannan were evaluated as indicated in Table 2.1. Os, laminarin, and mannan solutions were prepared in 10 mM NaP buffer (pH 7.4). All experiments were carried out at 30°C with the reference cell power set at 6 μ cal/sec. A total of 20 injections were done per experiment with a 2 μ L volume of laminarin/mannan per injection. The time between each injection was 120 sec with each injection taking 4 sec. The solutions were stirred at 600 rpm. Temperature changes were measured using Origin 7.0 software (Originlab Corporation, Northampton, USA) and the binding kinetics between Os and laminarin or mannan was evaluated.

Table 2.1: The different concentrations of Os used in ITC with the corresponding concentrations of laminarin and mannan used as titrant.

Os (μM)	Laminarin ($\mu\text{g/mL}$)	Relative μM	Mannan ($\mu\text{g/mL}$)	Relative μM	Estimated molar ratio (Os:polysaccharide)
1.2	12.1	24.0	16.0	24.0	1:20
12.0	242.0	480.0	319.0	480.0	1:40

2.9 Cell wall components binding assay

The modified microbroth dilution assay was used to determine whether Os interacts with different cell wall components of *C. albicans* in a biological environment. Os at its MIC of 10 μM , was mixed with 2X serial dilutions of mannan or laminarin (0.267 mg/mL, 0.202 mg/mL), respectively, and after an incubation time of 1 hour was added to *C. albicans* cells prepared as described in section 2.4. Exposure was for three hours and cell viability was determined using the CTB assay as described in section 2.4.1.

2.10 Membrane depolarization assay

An important function of the plasma membrane is to regulate the uptake and release of sodium- and potassium ions. Differences in ion concentrations across the plasma membrane create the membrane potential and if disrupted, can lead to cell death. DiBAC₄(3) is a fluorescent dye that, under normal conditions is unable to cross the cell membrane. Due to the overall negative charge of DiBAC₄(3), it is able to cross depolarized cell membranes (Figure 2.5) and localize to the cytosol.

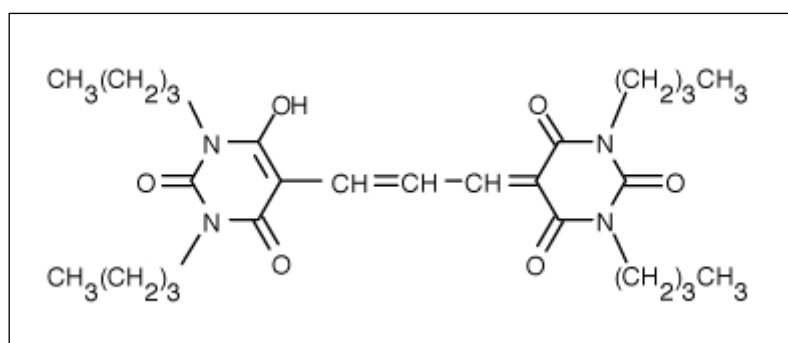


Figure 2.7: The chemical structure of protonated bis-(1,3-dibutylbarbituric acid) trimethine oxonol [DiBAC₄(3)]. This molecule is unable to cross the cell membrane due to its negative charge but once the cell membrane is depolarized, the molecule can cross the membrane and enter the cell (Brune *et al.*, 2002).

Melittin was used as a positive control as previous studies have shown its ability to cause membrane depolarization (Toraya *et al.*, 2005). For comparative purposes, the IC₅₀ of melittin was determined using the modified microbroth dilution assay as described in section 2.4.

The ability of Os compared with melittin to cause membrane depolarization in *C. albicans* was determined. The method described by Zoric *et al.* (2017) with minor modification was used. To determine membrane depolarization, cells were treated with 0.31 – 10 µM melittin or Os for 2 hours. Afterwards, 20 µL of DiBAC₄(3) (12 µg/mL) was added to cells for 1 hour. Thereafter the cells were washed with 1X phosphate-buffered saline (PBS; pH 7.4) to remove any excess dye, and the cells were collected with centrifugation (5000 x g, 10 min), and fluorescence was measured at an Ex of 488 nm and an Em of 510 nm.

2.11 Intracellular co-localisation of FAM-Os and vacuole staining

The uptake of Os into *C. albicans* cells is energy dependent (unpublished results) alluding to processes such as endocytosis. The possible association of endocytosis with vacuoles (Figure 1.6) and the effect of Os on vacuoles were determined.

The localisation of FAM labelled Os was determined at the IC₂₅ and IC₇₅ of Os. 5-Carboxyfluorescein (5-FAM) (Figure 2.7A) is a single isomer of carboxyfluorescein that contains a carboxylic acid, which can react with primary amines and is used as a green fluorescent tag to label peptides and proteins. In this study 5-FAM labelled penetratin (10 µM) was used as the control as previous studies (Alves *et al.*, 2011) have shown that penetratin enters *C. albicans* cells. 7-Amino-4-chloromethylcoumarin, known as CellTracker Blue-CMAC (CTB-CMAC) (Figure 2.7B) interacts with lipid bilayers and in an environment with reduced pH, such as vacuoles, will show strong blue fluorescence.

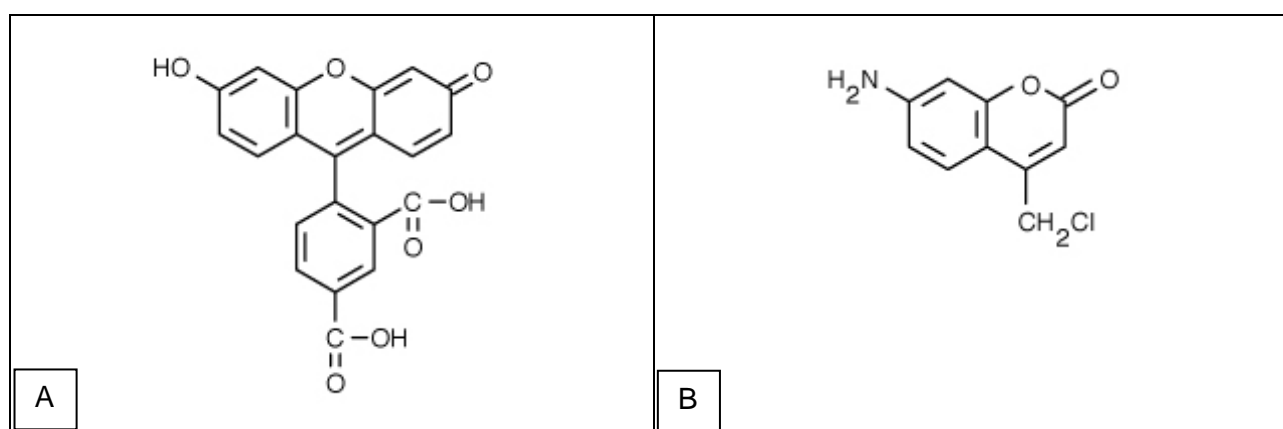


Figure 2.7: (A) Chemical structure of 5-carboxyfluorescein (5-FAM) that contains a carboxylic acid that can be used to react with primary amines via carbodiimide activation of the carboxylic acid and is used to fluorescently label peptides. (B) Chemical structure of 7-amino-4-chloromethylcoumarin, known as CellTracker Blue (CTB-CMAC) (ThermoFisher Scientific) which interacts with lipid bilayers and in environments with low pH such as vacuoles has blue fluorescence.

The co-localisation of FAM-Os and CTB-CMAC in the vacuoles of *C. albicans* was evaluated using flow cytometry and CLSM, based on the method described by Gong and Karlsson (2017) with some modifications. Flow cytometry as used in this study, provides quantitative information while CLSM provides qualitative information on the localisation and distribution of staining in an intracellular milieu.

Flow cytometry is an analytical method that allows the separation and analysis of single cells in suspension. Cells move in single file through a small channel as an excitation laser passes light of a specific wavelength through each cell (fluidic system). Detectors then measure forward scattered, side scattered and fluorescent light from each cell (optical system). This can then be analysed with software and generated data can provide information on the size and shape of cells or the amount of fluorescence of a specific fluorescence probe (electronic system) (Shapiro, 2005)(Figure 2.8).

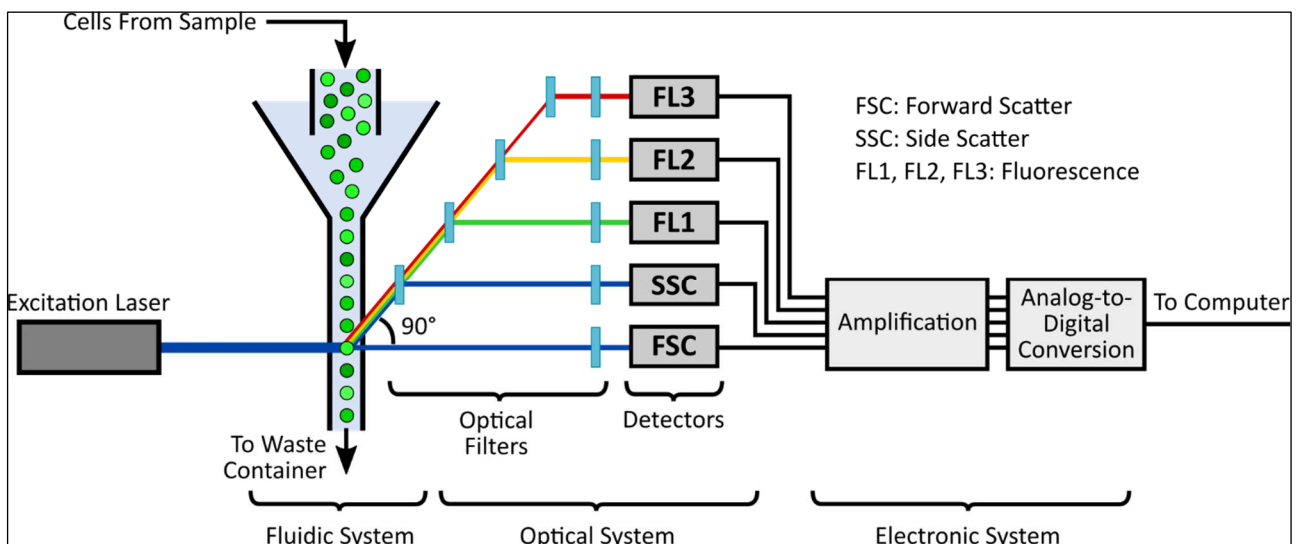


Figure 2.8: Basic layout of a non-cell sorting flow cytometer. The system is divided into three main sections the fluidic, optical and electronic systems (Castillo-Hair, 2016).

CLSM was used to evaluate the intracellular localisation of staining in *C. albicans*. In this type of microscopy, pinholes block out-of-focus light from above and below the focus point (Figure 2.9). This improves the quality of an image as all unfocused light is blocked from the detector but reduces the amount of light seen on the final image. The reduction in light is compensated for by using lasers, which provides high intensities of light, and photomultiplier-detectors, which helps to pick up reduced light signals. This is particularly useful in fluorescent microscopy as it is common to have unfocused fluorescent light in thicker samples with multiple focus planes. Due to the highly focused light on a sample, fluorescent bleaching can occur, and this is prevented by using small pulses of light rather than a continuous beam of light. Additionally, lasers emitting wavelengths of light are used in conjunction to create multi-coloured images of samples labelled with different fluorescent probes.

Certain software also allows the construction of 3-dimensional fluorescent images by combining images from different focal planes (Nwaneshiudu et al., 2012, Spring, Fellers and Davidson, 2012).

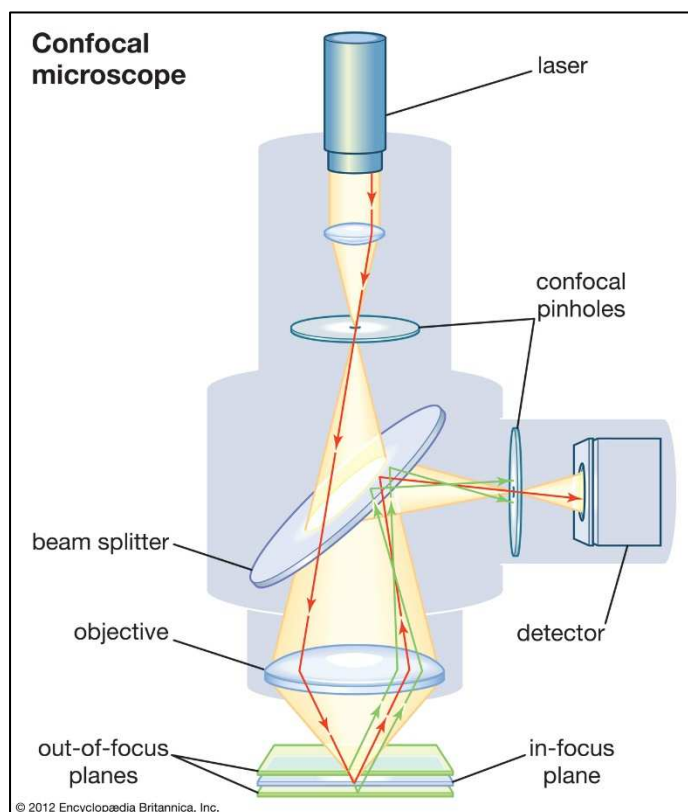


Figure 2.9: Excitation and emission light pathways in a scanning confocal laser microscope configuration. Unfocused light is blocked from the detector to allow focus on a specific plane of a sample. This allows visualization of thicker samples compared to standard fluorescent microscopes (Desig.kristinejaynephography.com, 2020).

Planktonic *C. albicans* cells were treated with 0.5 μM and 6.3 μM Os, fluorescently labelled with 5-FAM at the N-terminal under the same conditions described for the modified microbroth dilution assay (Section 2.4). After 1 hour of treatment in Eppendorf tubes, the cells were washed with NaP (10 mM, pH 7.4) and were collected with centrifugation at 5000 x g for 10 min. The cells were incubated with 0.025% trypsin (Merck, RSA) for 10 min to remove any attached extracellular peptide (Muñoz *et al.*, 2012). After staining with CTB-CMAC for 40 min, the cells were resuspended in NaP buffer (10 mM, pH 7.4) and analysed with flow cytometry (BD FACSAria Fusion, BD Biosciences, Johannesburg, RSA).

For SLCM live cells were plated onto poly-L-lysine covered coverslips which were then inverted onto sterile glass slides and sealed using colourless nail polish. The samples were visualized within 12 hours after being added onto cover slips, using a SLCM (Zeiss, Oberkochen, Germany). Images were analysed using AXIO VISION 4.8 software (Zeiss, Oberkochen, Germany).

2.12 Statistical analysis

Data are representative of three independent experiments performed in duplicate or triplicate as indicated. Data was analysed using the GraphPad Prism 6 software program. Multiple comparisons were tested by two-way ANOVA followed by the Tukey's post hoc test to obtain statistical significance of $p < 0.05$ when necessary. Inhibitory activity values are represented by the mean \pm standard error.

3 Results

3.1 Modified microbroth dilution assay

Os loses activity in complex media with high salt concentrations (Mbuayama, 2016). Therefore, a modified version of the microbroth dilution assay was developed to determine the activity of Os against planktonic *C. albicans*. For optimization, *C. albicans* cells were grown in 100% - 1% dilutions of RPMI diluted with NaP buffer. The lowest dilution that supports the growth of *C. albicans* similar to growth in 100% RPMI was determined. In Figure 3.1, 10% RPMI/NaP was identified as the lowest dilution where there was no significant difference between the viability of cells compared to cells in 100% RPMI. Cells grown in the different dilutions of RPMI/NaP were exposed to AmpB to determine if the sensitivity of *C. albicans* to an antimicrobial agent is altered when grown in media with a reduced nutrient content. No significant difference in viability between cells treated with AmpB at the different dilutions of RPMI/NaP was observed indicating no changes in sensitivity.

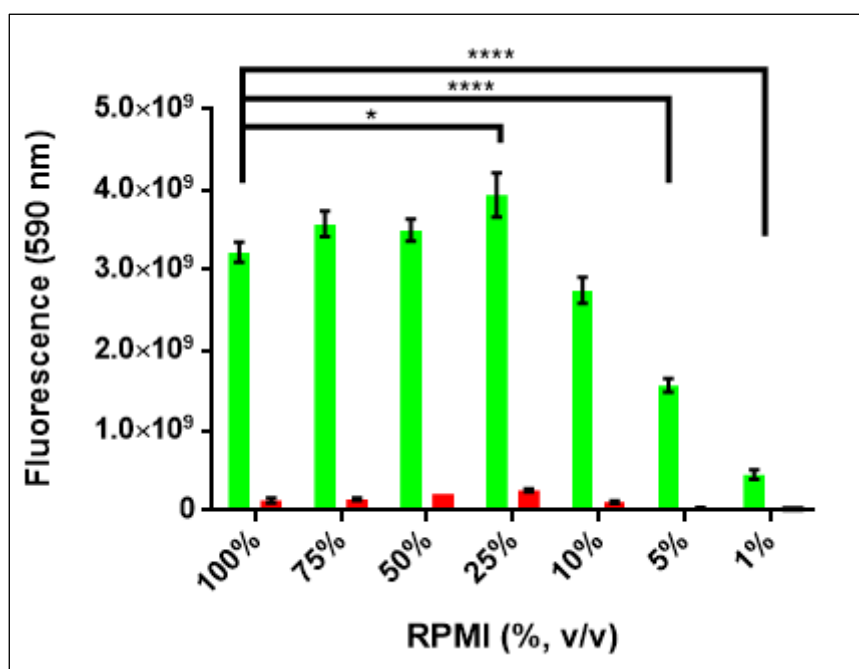


Figure 3.1: Fluorescence as a measure of the viability of planktonic *C. albicans* cells grown in different dilutions of RPMI/NaP with/without 2.5 μ M AmpB. Green bars measured fluorescence for *C. albicans* grown in different dilutions of RPMI/NaP. Red bars represent the fluorescence of *C. albicans* grown in different dilutions of RPMI/NaP exposed to AmpB at its MIC of 2.5 μ M. Significant differences are indicated by (*, **, ***, ****) where $p < 0.05, 0.01, 0.001$ and 0.0001 .

3.2 Inhibitory activity of Os

At a lower media dilution of 10% RPMI, the modified version of the microbroth dilution assay could be used to determine the activity of Os using AmpB as a positive control. The IC_{50} for AmpB was $0.547 \pm 0.056 \mu$ M and for Os was $1.163 \pm 0.116 \mu$ M (Figure 3.2). Melittin was used as a positive

control in membrane depolarization studies. The IC_{50} of melittin was $1.08 \pm 0.07 \mu\text{M}$ (Figure 3.2C). From these curves the IC_{25} , IC_{50} and IC_{75} values were calculated (Table 3.1) and were used for further mode of action studies.

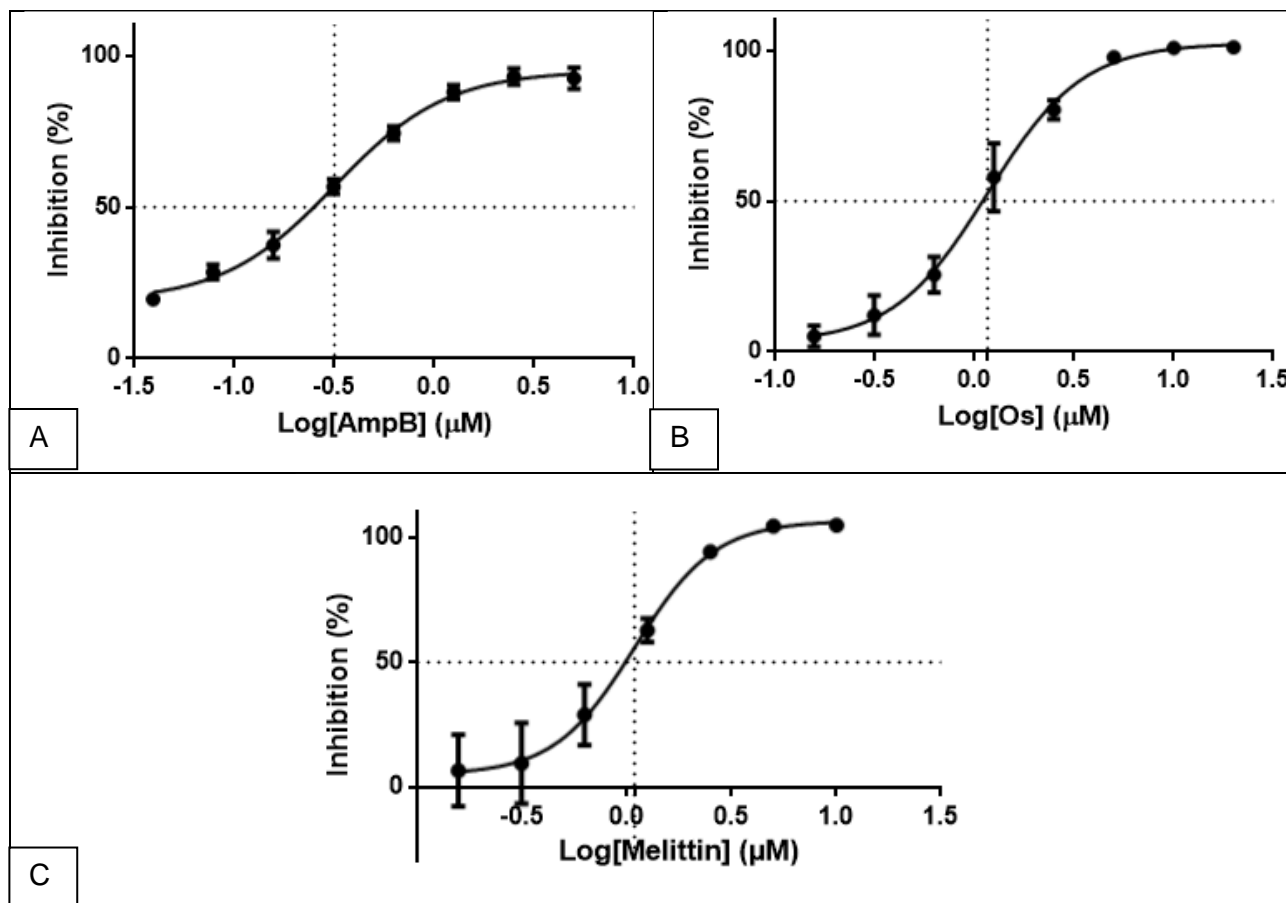


Figure 3.2: The activity of (A) AmpB (positive control), (B) Os and (C) melittin against planktonic *C. albicans* cells after 3 hours treatment determined with the modified microbroth dilution assay. AmpB has an IC_{50} of $0.547 \pm 0.056 \mu\text{M}$, Os has an IC_{50} of $1.163 \pm 0.116 \mu\text{M}$ and melittin has an IC_{50} of $1.08 \pm 0.07 \mu\text{M}$. Graphs are representatives of three independent biological repeats. The IC_{50} values represent the mean \pm standard error of the mean of three independent biological repeats.

Table 3.1: The IC_{25} , IC_{50} and IC_{75} of AmpB and Os against *C. albicans* growth. The IC_{50} of the control melittin is included.

Treatment	IC_{25}	IC_{50}	IC_{75}
AmpB*	$0.150 \pm 0.076 \mu\text{M}$	$0.547 \pm 0.056 \mu\text{M}$	$1.101 \pm 0.062 \mu\text{M}$
Os*	$0.561 \pm 0.086 \mu\text{M}$	$1.163 \pm 0.116 \mu\text{M}$	$6.350 \pm 0.057 \mu\text{M}$
Melittin*	$0.625 \pm 0.103 \mu\text{M}$	$1.08 \pm 0.070 \mu\text{M}$	$1.65 \pm 0.056 \mu\text{M}$

*Values represent the mean \pm standard error of the mean of three independent biological repeats.

3.3 Effect of Os on *C. albicans* ultrastructure

The effects of Os and AmpB at concentrations equal to their IC₂₅, IC₅₀ and IC₇₅ values (Table 3.1) on the external ultrastructure of planktonic *C. albicans* were evaluated with SEM (Figure 3.3). Control cells have a typical oval shape and a smooth outer surface that represents the typical morphology of *C. albicans*. At the IC₂₅ of AmpB the cell shape is irregular, the cell wall is not as smooth compared with the control. At the IC₅₀ small evenly dispersed extracellular vesicles (EV) are present on the cell wall. Pits (white arrows) and bud scars (red arrows) are also present. There are also signs of extravasation of cellular contents (blue arrows). At the higher concentration, IC₇₅, the cells are elongated, with a ruffled surface and filamentation occurring.

At the IC₂₅ of Os, the morphology of *C. albicans* is altered and there are small pits on the cell wall. Bud scars are also present and appear elongated. Fewer cells appear to be spherical compared to untreated cells, with more elongated and tube-like cell formations. There appears to be extravasation of cellular contents (blue arrow). Exposure to Os at the IC₅₀ causes the cell membrane to be irregular with indentations (white arrows) and small blebs. Cells also appear to separate irregularly with clear scars appearing where the mother and daughter cell used to be attached (white circles). At the IC₇₅, the cells are flattened with large pseudopodia-like structures, large pores are present (white arrows), and the scar bud appears to be shrivelled (red arrows). Pits on the surface of the cell also appear to become larger. Budding on the cell surface appear to be more numerous compared to cells treated with lower concentrations of Os. Morphological features indicated that the effect of Os is different from that of AmpB.

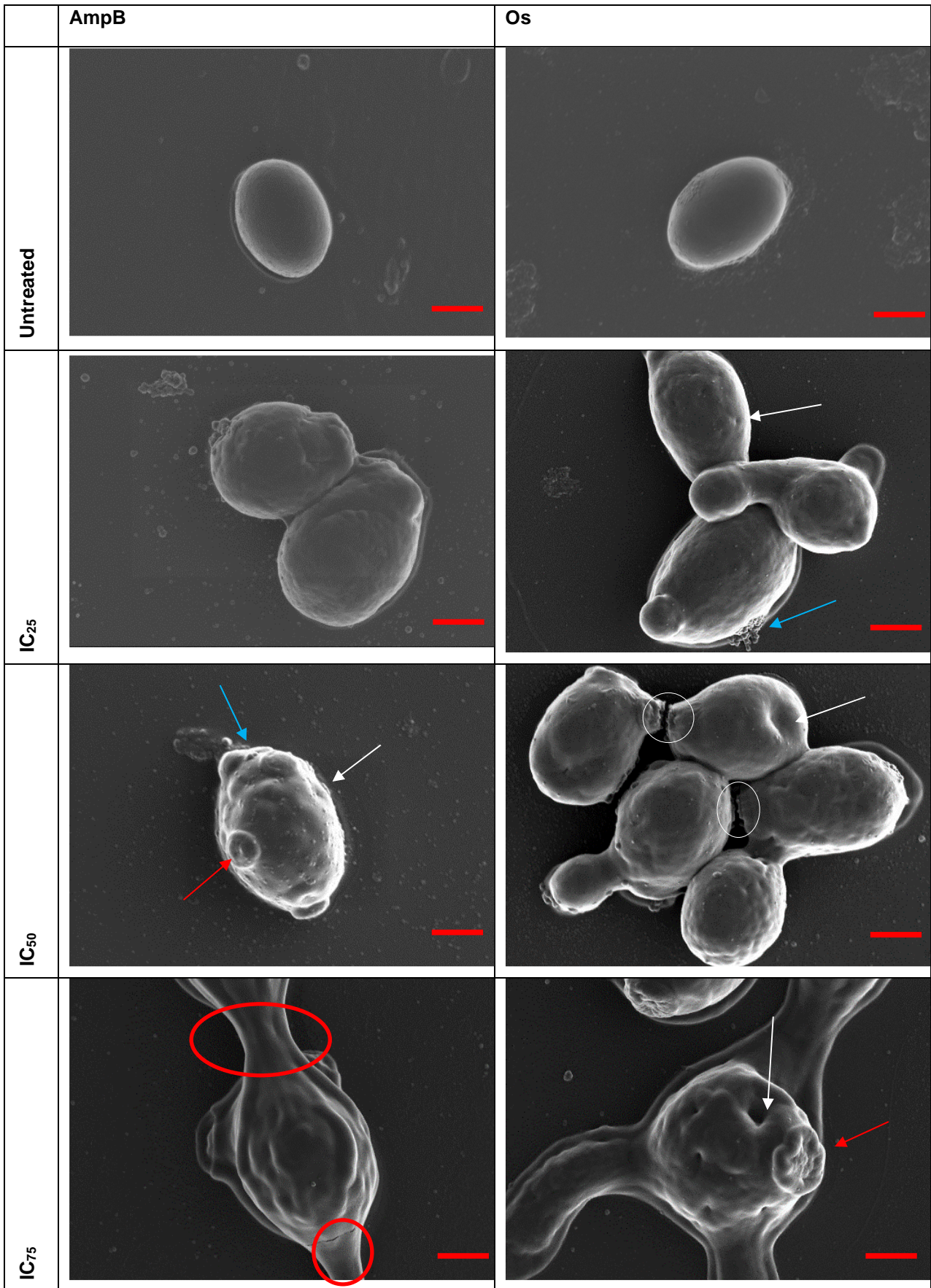


Figure 3.3: Scanning electron microscope images of planktonic *C. albicans* treated for 3 hours with AmpB or Os at concentrations equal to the IC₂₅, IC₅₀ and IC₇₅. Images shown are representatives of the majority of cells seen for each sample. White arrows indicate pits on the cell wall surface. Red arrows indicate budding scars. Blue arrows indicate extravasation of cellular contents. Red circles indicate germ tubes caused by filamentation of cells. Scale bars represent 1 μ m.

The effects of Os on the ultrastructure of planktonic *C. albicans* cells were further investigated using TEM. This allowed visualization of the cell wall and membrane and the intracellular structure of *C. albicans*. AmpB was used as a positive control again as its effects on *C. albicans* is well studied.

Untreated *C. albicans* cells have a regular rounded shape with a clearly defined cell membrane and cell wall with fibrils (Figure 3.4). Exposure to AmpB appears to affect the cell morphology in a dose-dependent manner. With increasing concentrations, the cell shape changes from a regular round to ovoid to a sickled shape. Fibrils are absent and the thickness of the cell wall varies from being thin (yellow arrows) to being thick (black arrows). The cell membrane is irregular (red arrows), and in some areas is absent or breaking away from the cell wall (blue arrows). With exposure, the organelles, such as vacuoles and nuclei, are localized at the inner curve or concave surface. The nucleus appears to be breaking apart similar to how the cell membrane is breaking away from the cell wall, with clear pores appearing.

Likewise, the intracellular effects of Os at concentrations equal to the IC₂₅, IC₅₀ and IC₇₅ on planktonic *C. albicans* cells were analysed using TEM. Figure 3.5 shows representations of the populations of cells in each sample. The untreated control cell had a typical oval shape with a bud scar, a light staining nucleus and dark staining vacuole. Both the cell wall and cell membrane are smooth and regular. With exposure, the oval, rounded shape is retained and the cell wall and cell membrane remained regular when compared with the effects of AmpB. Cells treated with Os show cytosolic retraction from the cell wall (blue arrows). The cytoplasm of cells treated with the IC₂₅ and IC₅₀ of Os appear to be more electron dense while exposure to the IC₇₅ resulted in a cytoplasm with a regular wavy appearance (red circle) and is possibly due to the precipitation of cytosol contents, such as proteins. Finally, there seems to be an increase in budding compared to untreated cells (red arrows) and may be due to filamentation as observed with SEM.

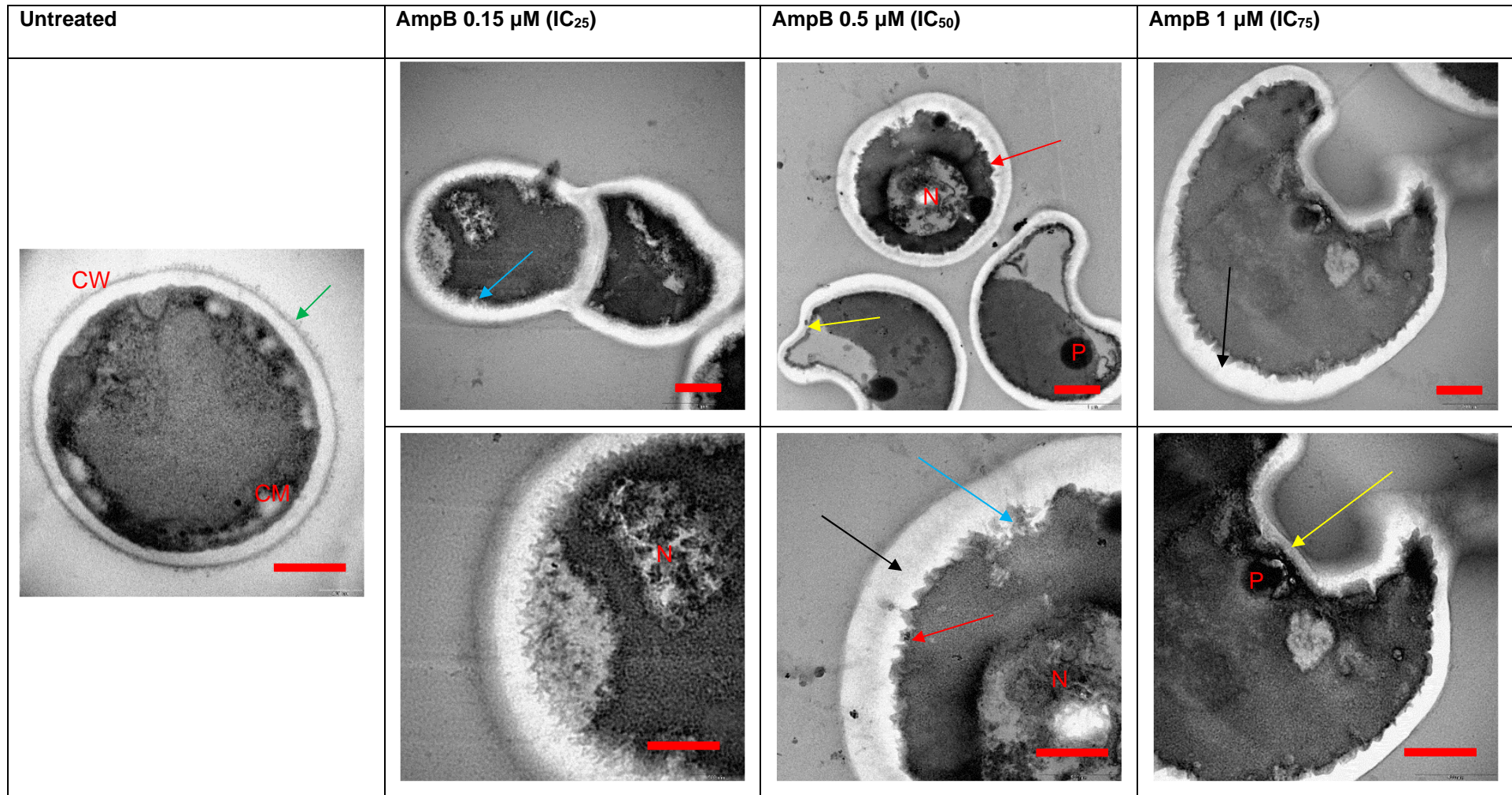


Figure 3.4: Transmission electron microscope images at different magnifications of planktonic *C. albicans* cells treated with different concentrations of AmpB. In the untreated control, fibrils (green arrow), a regular cell wall (CW) and cell membrane (CM) are present. With exposure to AmpB the cell shape becomes sickled shape. Fibrils are absent and the cell wall thickness varies from being thin (yellow arrows) to being thick (black arrows). The cell membrane is irregular (red arrows) with some areas being absent or breaking away from the cell wall (blue arrows). Organelles, such as vacuoles and nuclei, localize on the concave surface. Small scale bars indicate 1 μ m and large scale bars indicate 200 nm. (V: vacuole, P: peroxisomes, N: nucleus)

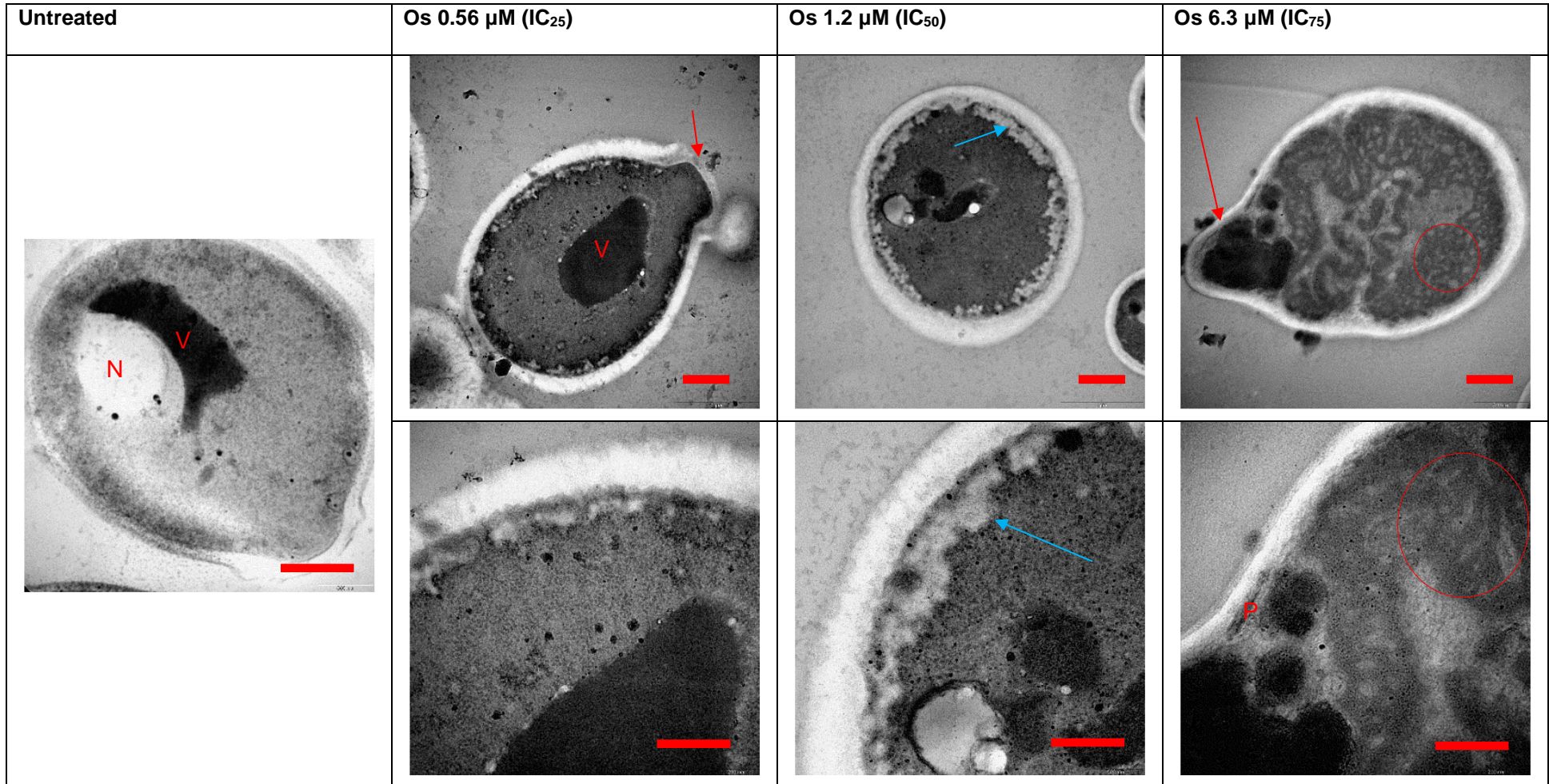


Figure 3.5: Transmission electron microscope images of planktonic *C. albicans* cells treated at the IC_{25} , IC_{50} and IC_{75} of Os. Exposure causes cytosolic retraction from the cell wall (blue arrows). At the IC_{25} and IC_{50} , the cytoplasm is more electron dense and remaining cells at IC_{75} have a regular wavy appearance (red circle). The number of bud scars are increased (red arrows). Small scale bars indicate 1 μm and large scale bars indicate 200 nm. (V: vacuole, P: peroxisomes, N: nucleus)

3.4 Interactions with cell wall components

Before evaluating the interactions between Os and mannan or laminarin with ITC, a positive and negative control was tested. As a positive control, ethylenediaminetetraacetic acid (EDTA) with calcium carbonate (CaCO_3) was used (Figure 3.6). A typical curve of molar ratio and $\mu\text{cal}/\text{sec}$ was obtained due to the strong interaction between EDTA and CaCO_3 observed at a molar ratio of approximately 1:1. Both mannan and laminarin alone in buffer did not cause any interference, except for a single peak signal in the mannan/buffer control, which was most likely due to an air bubble escaping the solution.

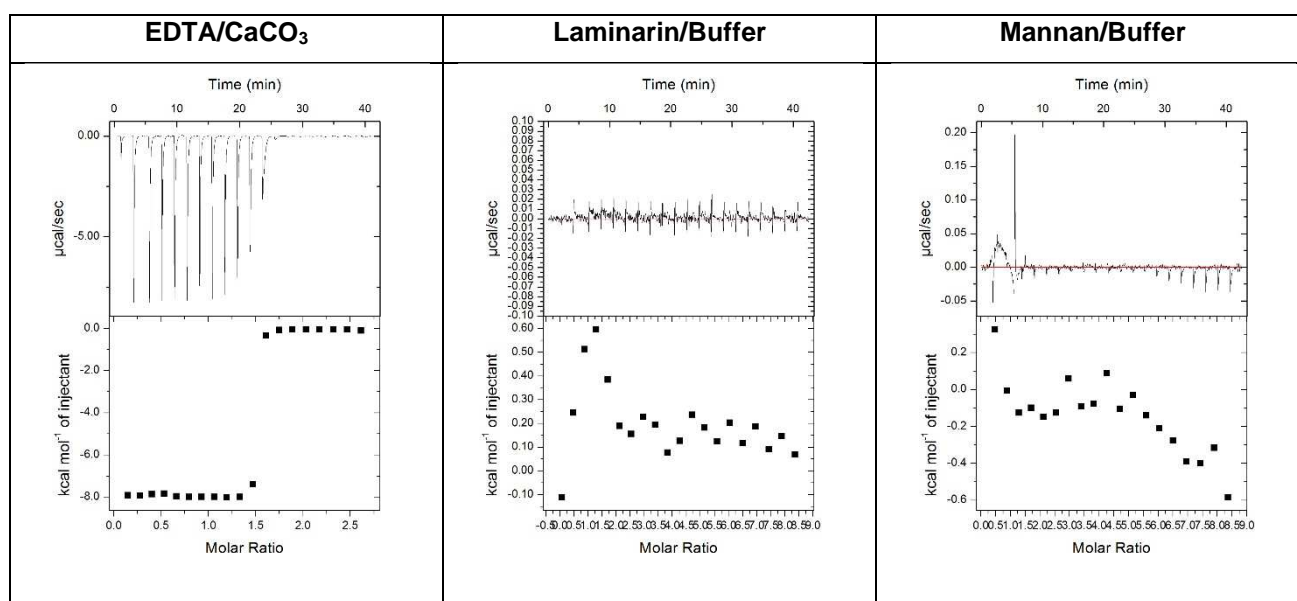


Figure 3.6: Titration graphs indicating heat changes from mannan or laminarin mixed with buffer and EDTA interacting with CaCO_3 respectively.

Then the interaction of Os with mannan and laminarin, was performed (Figure 3.7). Os was first tested at its IC_{50} with mannan and laminarin concentrations in the syringe being 20X higher than the IC_{50} of Os (estimated ratio 1:20). No significant heat changes that were greater than the background were observed.

To confirm the lack of interaction between Os and mannan or laminarin, the concentrations were increased. For these experiments Os was tested at 10X higher concentrations than the IC_{50} and the concentrations of mannan and laminarin were increased to 40X the concentration of Os (estimated ratio 1:40). Even at the higher concentrations and molar ratios, no significant interactions were observed. Therefore, under these conditions no binding occurred.

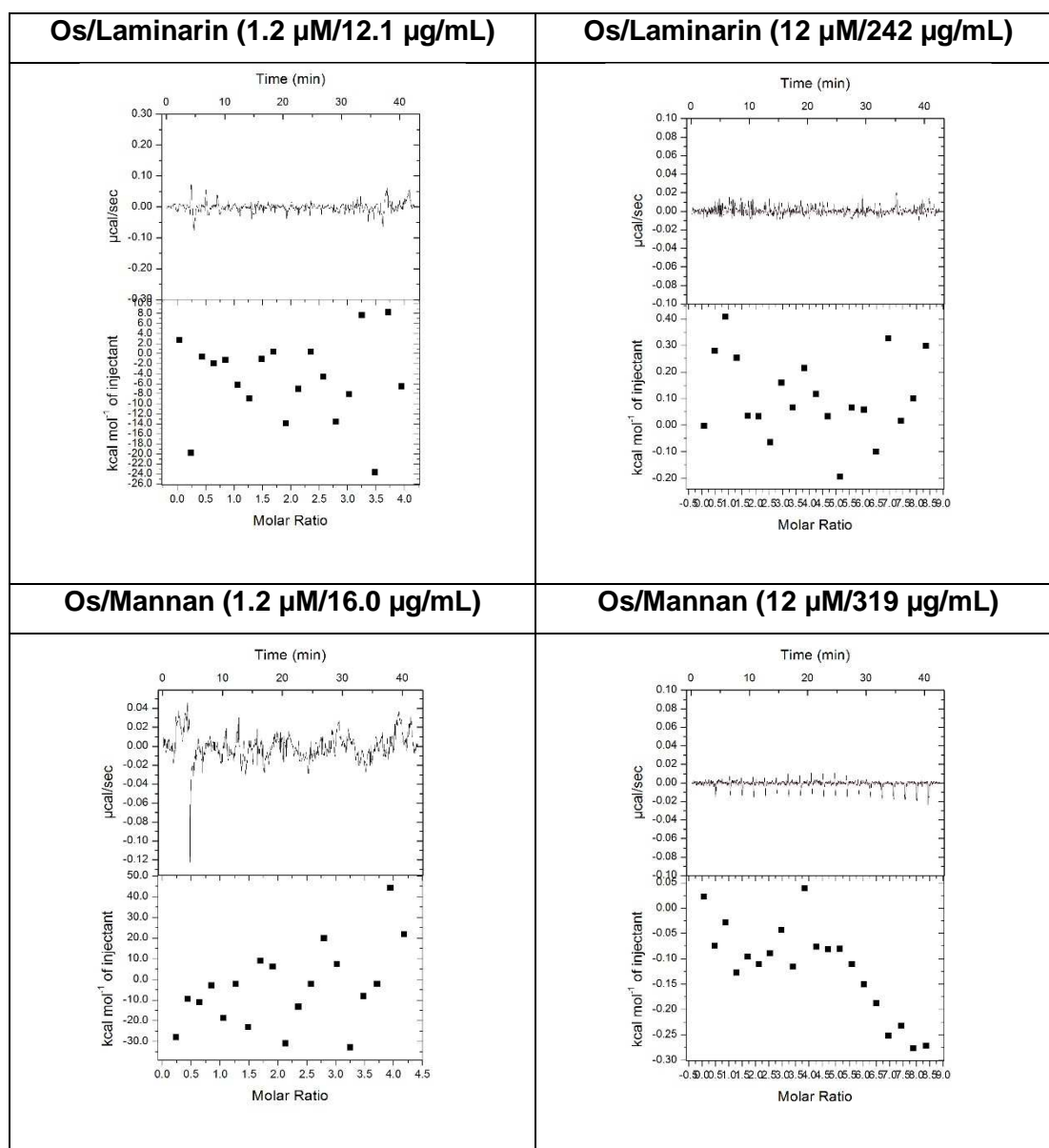


Figure 3.7: Titration graphs indicating heat changes due to interactions between Os and mannan and laminarin respectively. The graphs are representatives of three independent repeats for each titration. At the lower concentrations (left) Os was tested at its IC₅₀ with mannan and laminarin concentrations within the syringe being 20X higher than Os. At higher concentrations Os was tested at 10X its IC₅₀ with mannan and laminarin concentrations in the syringe being 40X higher than Os.

After ITC showed that there is no binding between Os and mannan or laminarin, the microbroth dilution assay in the presence of mannan or laminarin was performed. This was undertaken to determine if the interaction between Os and the cell wall components are dependent on a cellular environment. In the presence of increasing concentrations of laminarin and mannan, the antifungal activity of AmpB was unaltered (Table 3.2). At the concentrations of laminarin and mannan used for ITC there were no changes in the antifungal activity of Os. However, when the concentrations of mannan and laminarin were increased to 20 mg/mL, there was a $34,0 \pm 13,9\%$ and $35,6 \pm 14,5\%$ reduction in Os activity, respectively.

Table 3.2: Inhibitory activity of Os and AmpB at their respective IC₅₀ values against planktonic *C. albicans* in the presence of increasing concentrations of mannan and laminarin.

Laminarin (mg/mL)	Inhibition (%)		Mannan (mg/mL)	Inhibition (%)	
	AmpB (2.5 μ M)	Os (10 μ M)		AmpB (2.5 μ M)	Os (10 μ M)
0	87,1 \pm 0,88	100 \pm 0,32	0	87,1 \pm 0,88	100 \pm 0,32
0,003	90,5 \pm 1,12	99,5 \pm 1,92	0,004	94,6 \pm 1,06	99,4 \pm 0,23
0,006	89,3 \pm 3,50	99,3 \pm 1,60	0,007	94,2 \pm 0,14	99,6 \pm 0,59
0,013	88,8 \pm 4,30	99,5 \pm 1,65	0,017	93,2 \pm 1,11	99,5 \pm 0,46
0,025	87,9 \pm 4,79	99,4 \pm 1,51	0,033	89,4 \pm 3,76	99,6 \pm 0,49
0,050	83,1 \pm 9,17	99,6 \pm 1,63	0,067	88,1 \pm 6,49	99,5 \pm 0,48
0,100	89,4 \pm 3,96	99,3 \pm 1,50	0,133	87,7 \pm 6,68	99,5 \pm 0,36
0,202	89,9 \pm 3,31	99,4 \pm 1,47	0,267	89,9 \pm 5,18	99,7 \pm 0,90
20	100 \pm 0,13	34,0 \pm 13,9*	20	83,8 \pm 3,45	35,6 \pm 14,5*

Values represent the mean \pm standard error of the mean of three independent biological repeats. *Two-way Anova comparisons between 20 mg/mL of mannan or laminarin and lower concentrations show that there is a significant difference in the antifungal activity of Os.

3.5 Membrane depolarization

The antimicrobial activity of several AMPs is due to membrane depolarization (Graf *et al.*, 2017). To investigate whether the antifungal activity of Os is a result of membrane depolarization, the fluorescent dye DiBAC₄(3) was used. Melittin served as a positive control as this peptide has shown membrane depolarization activity in bacterial and fungal cells (Toraya *et al.*, 2005).

DiBAC₄(3) is unable to cross polarized membranes, but with increasing concentrations of melittin there was a linear increase in fluorescence, indicating membrane depolarization (Figure 3.8A). For Os a sigmodal increase in fluorescence was observed (Figure 3.8B) indicating that Os requires higher concentrations and there is a critical threshold before membrane depolarization occurs. At the IC₅₀ of melittin, 1.0 x 10⁷ fluorescence units were measured while at the IC₅₀ of Os less than 1.0 X 10⁶ fluorescence units were measured. Melittin appears to cause depolarization at concentrations as low as 0.63 μ M while Os was only able to start depolarizing membranes at 2.5 μ M. Therefore, compared to melittin these results suggest that the antifungal activity of Os is not due to membrane depolarization.

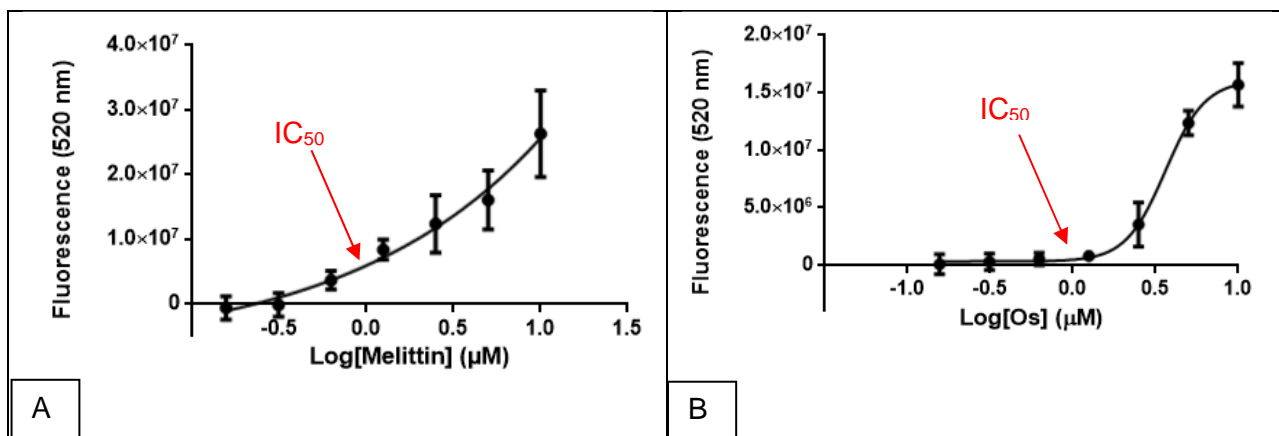


Figure 3.8: The amount of membrane depolarization caused by different concentrations (0.15-10 μM) of (A) melittin and (B) Os in *C. albicans* membranes. Membrane depolarization was quantified by measuring intracellular fluorescence emitted by DiBAC₄(3). Graphs represent three independent biological repeats presented as the mean \pm standard error of the mean.

3.6 Intracellular localisation

To evaluate whether Os targets vacuoles by targeting the cell membrane or by disrupting pathways associated with the vacuoles, flow cytometry was used. Quadrants were calibrated using untreated, both stained and unstained, planktonic *C. albicans* (Figure 3.9). As expected, cells treated with free 5-FAM did not contain intracellular 5-FAM fluorescence.

The untreated control and free 5-FAM control stained positively for CTB-CMAC (85.11% and 85.06%, respectively), indicating vacuole staining. Cells treated with 5-FAM-penetratin showed strong fluorescence with 99.89% of cells being positive for FAM-penetratin. Only 0.08% of the cell population was positive for both 5-FAM-penetratin and CTB-CMAC indicating that 5-FAM-penetratin enters planktonic *C. albicans* cells, accumulates in the cytoplasm and breaks down intracellular membranes.

Cells treated with 0.5 μM 5-FAM-Os have a strong fluorescent signal of 73.42% for both 5-FAM-Os and CTB-CMAC with 26.42% of the cell population staining for only 5-FAM-Os, indicating that at lower concentrations Os is able to enter cells but does not break down intracellular membranes. At 6.3 μM , 5-FAM-Os and CTB-CMAC staining decreased to 3.78% and 5-FAM-Os staining increased to 96.17%, indicating that at higher concentrations Os starts to enter cells more effectively and break down intracellular membranes.

There is no significant difference in the number of cells positive for CTB-CMAC between untreated cells and cells treated with 0.5 μM Os (Figure 3.10). At the higher concentration Os, CTB-CMAC staining is reduced significantly with no significant change in the percentage of 5-FAM positive cells.

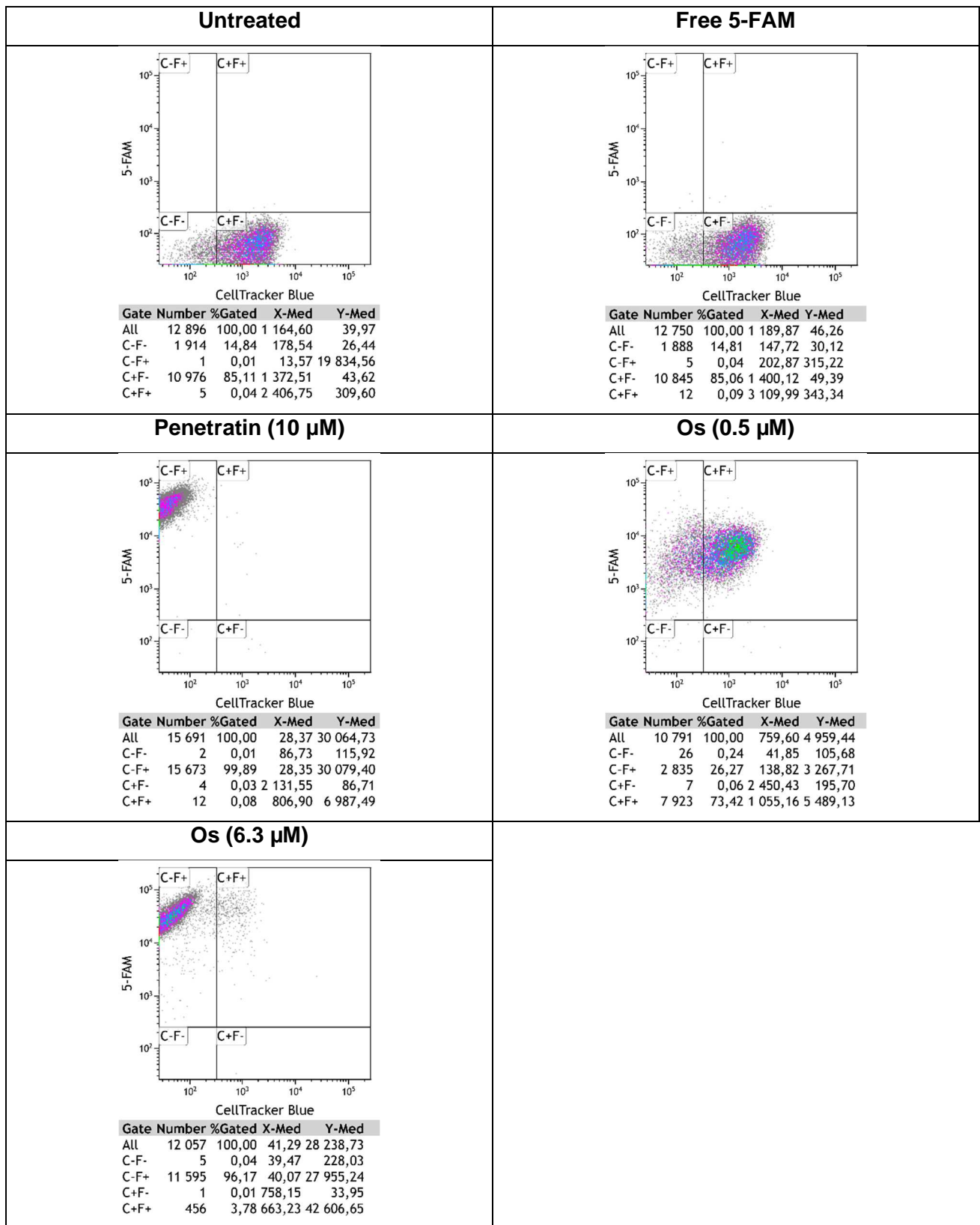


Figure 3.9: Scatterplot graphs of 5-FAM peptide and CTB-CMAC fluorescent signals obtained from flow cytometry. Quadrants are CF+, only 5-FAM peptide, C+F- only CTB-CMAC staining, and C+F+ both 5-FAM peptide and CTB-CMAC fluorescence. Below each scatterplot graph is a table indicating the cell count in each quadrant as well as the percentage cells relative to the total cell count. Scatterplots are representative of three independent biological repeats.

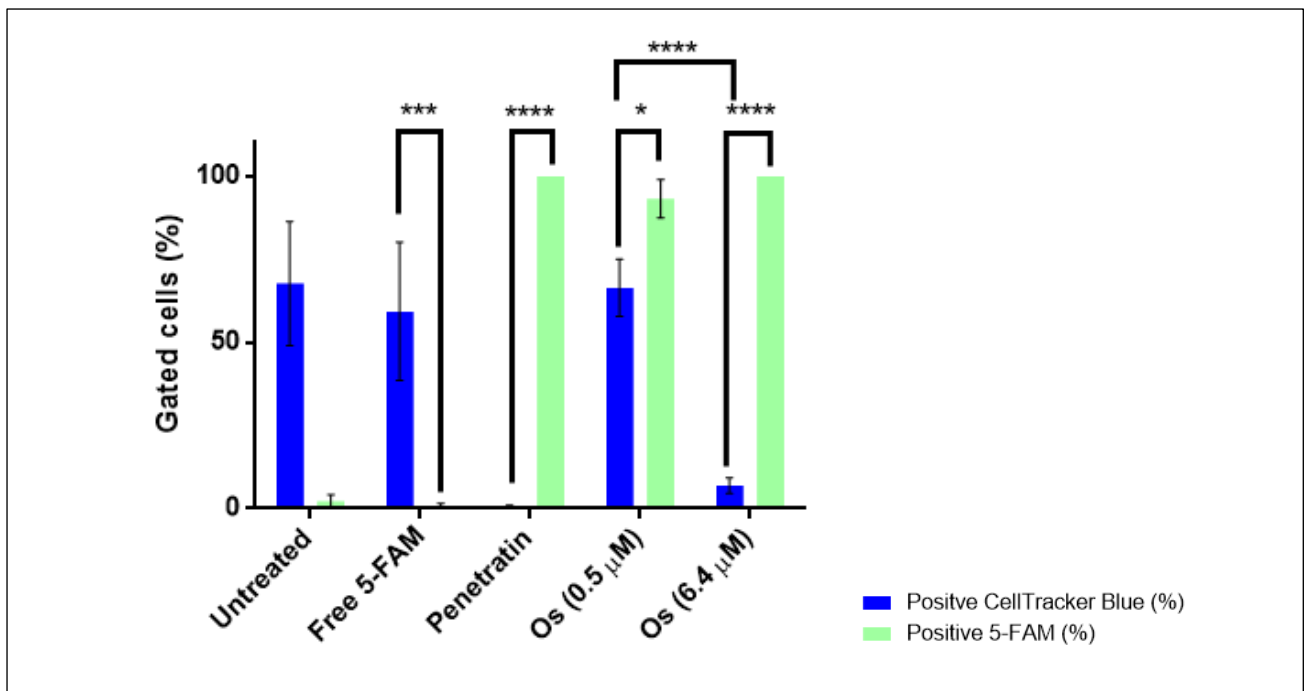


Figure 3.10: Percentage of total cells containing either CTB-CMAC or 5-FAM measured using flow cytometry for *C. albicans* cells treated with fluorescently labelled peptides. Blue bars represent the percentage cells positive for CTB-CMAC, including cells that contain 5-FAM-peptide. Green bars represent the percentage of cells positive for 5-FAM-Peptide, including cells stained with CTB-CMAC. Representation of 3 independent biological repeats. (*: $p < 0.05$, ***: $p < 0.001$, ****: $p < 0.0001$).

At a cellular level, the findings with flow cytometry were evaluated in more detail using CLSM. Planktonic *C. albicans* cells were exposed to the labelled 5-FAM peptides for 3 hours. The cells were then treated with trypsin to remove peptide attached to the cell surface before CTB-CMAC staining for vacuoles.

Figure 3.11 shows CLSM images of treated and untreated *C. albicans* cells stained with CTB-CMAC. Untreated cells showed some intracellular regions of blue fluorescence, indicating vacuole staining (red circles). Cells treated with 5-FAM-penetratin clearly showed intracellular 5-FAM signals (red arrows), indicating that penetratin successfully crosses cell membranes and with non-specific intracellular localisation as described in Gong and Karlsson (2017). Some cells also appear to still have both 5-FAM as well as vacuole staining (white arrows).

Cells treated with low concentrations of Os mostly showed fluorescence associated with the cell membrane (yellow arrows). At low concentrations, Os also appeared to localize in the nuclei with blue CTB-CMAC fluorescence staining of the vacuoles in different locations to 5-FAM-labeled Os (see insert). Cells treated with higher concentrations of Os have 5-FAM fluorescence throughout the cytoplasm indicating that Os crosses the plasma membrane and accumulates in the cytoplasm. Cells with higher intracellular accumulation of 5-FAM-Os also appeared to have lower CTB-CMAC fluorescence (red arrows). Some cells appeared to have a bright blue fluorescence. These cells are most likely less affected by Os, still containing viable intracellular membranes (white arrows).

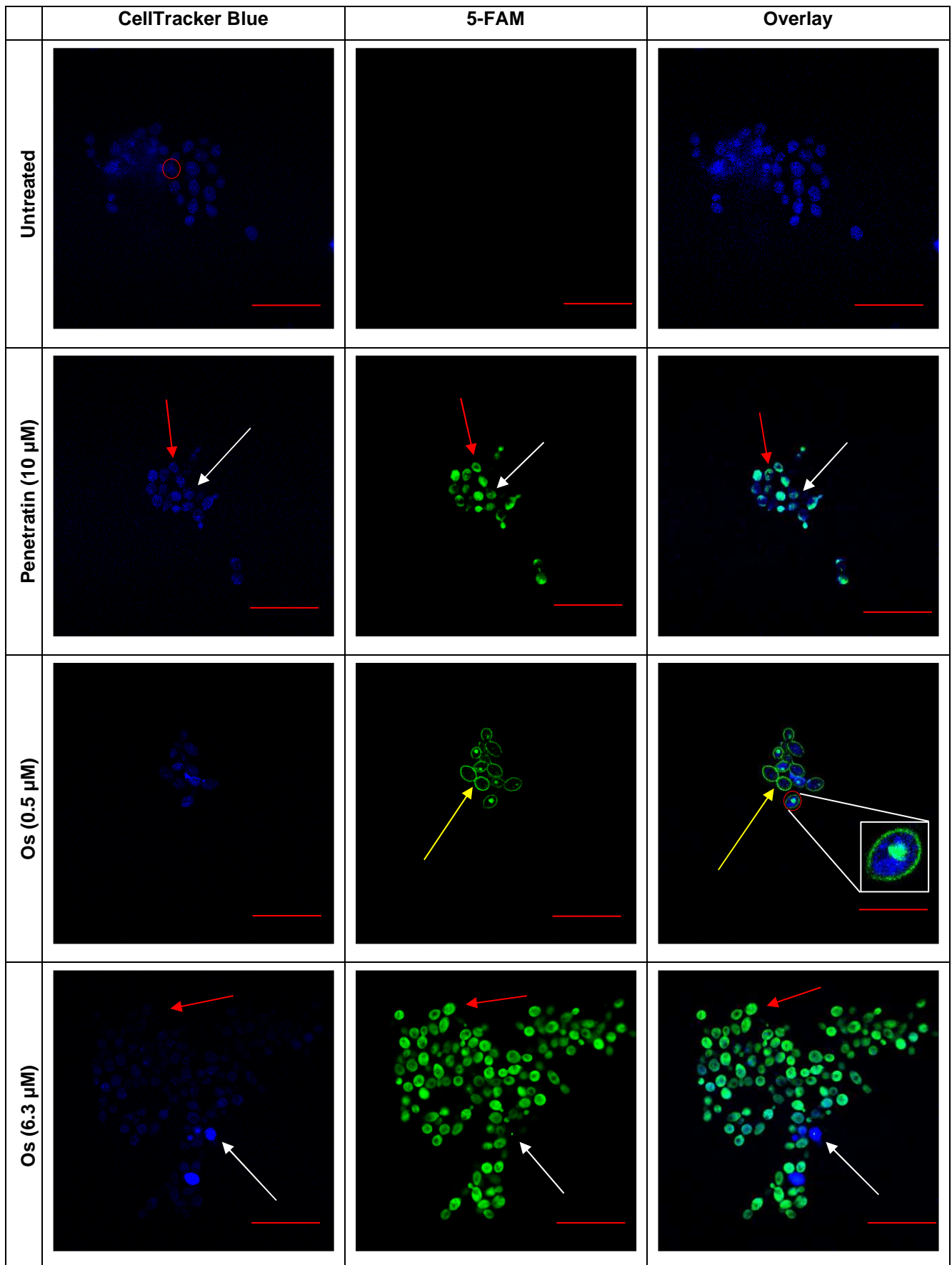


Figure 3.11: CLSM images of planktonic *C. albicans* cells stained with CellTracker Blue and treated with free 5-FAM and peptides (penetratin or Os) labelled with 5-FAM. Arrows indicate *C. albicans* cells that have cytoplasmic accumulation of peptide with vacuolar staining (white arrow), plasma membrane with 5-FAM peptide (yellow arrow) and cytoplasmic accumulation of 5-FAM-Os or 5-FAM-penetratin with no vacuole staining (red arrow). Scale bars represent 20 µm.

4 Discussion

Os is an antimicrobial peptide derivative of the defensin OsDef2, with activity against both Gram-positive and -negative bacteria, as well as the fungus *C. albicans* (Mbuayama, 2016, Taute, 2017). The aim of this study was to further investigate the different modes of action of the antimicrobial peptide Os in planktonic *C. albicans* cells.

Assays used to evaluate the antifungal activity of drugs, are the RDA and the colony forming unit assay used to determine the MIC and MFC, respectively. Both methods are time consuming and consequently the microbroth dilution assay was developed and has been used since the 1970's for the rapid testing of activity (Witebsky *et al.*, 1979). The advantages of this assay compared with traditional methods include being more cost-effective and less time-consuming (Testing, 2008). However, due to the salt sensitivity of many AMPs, including Os, the use of the microbroth dilution assay is limited. RPMI used for antifungal microbroth dilution assays is a complex medium of nutrients, salts, vitamins, amino acids at concentrations and pH that represents a physiological environment. The high salt content limits the use of the microbroth dilution assay for the rapid screening of AFPs. To overcome this limitation, the effects of growing *C. albicans* in media with a reduced RPMI content was evaluated. In this growth medium, it was necessary to determine if the growth and sensitivity of *C. albicans* cells to AmpB was the same as cells grown in 100% RPMI, as used in the microbroth dilution assay.

Planktonic *C. albicans* cells were grown in different dilutions of RPMI diluted with 20 mM NaP buffer (100% RPMI - 1% RPMI/NaP). After 3 hours incubation at 37°C, 10% RPMI/NaP resulted in growth and cell viability, measured with CTB similar to cells grown in 100% RPMI. Also, the fluorescent signal difference from CTB between untreated cells and cells treated with 5 µM AmpB was large enough to clearly distinguish between maximum and minimum signals when constructing inhibition curves. The percentage inhibition by 5 µM AmpB was similar for *C. albicans* grown in 100% RPMI and 10%RPMI/NaP indicating that in a medium reduced environment the sensitivity of the cells to AmpB had not increased.

Using the modified microbroth dilution assay, the IC₅₀ of AmpB was determined as 0.547 ± 0.056 µM and IC₅₀ of Os was found to be 1.163 ± 0.116 µM. The IC₅₀ of AmpB was similar to 0.26 ± 0.01 determined by Troskie *et al.* (2014) with the standard microbroth dilution assay. The IC₅₀ of Os is comparable to other peptides in literature tested against *C. albicans*, such as penetratin and pVEC with IC₅₀ values of 1 µM and 2 µM, respectively, evaluated with a microbroth dilution assay in YPD broth (Gong and Karlsson, 2017).

Using the modified microbroth dilution assay the IC₅₀ for melittin was determined as 1.08 ± 0.07 µM and has a reported MIC of 2.5 µM (Park and Lee, 2009). The IC₅₀ of melittin is very similar to that of Os but in contrast to melittin, Os is not cytotoxic to mammalian cells (Table 1.1). Therefore, the further

development of Os as an antifungal agent is of value. From the dose-response curves (Figure 3.8) the IC₂₅ and IC₇₅ values of Os and AmpB were calculated and these concentrations were used in the mode of action studies. An interesting observation was that Os has a higher IC₇₅ than both AmpB and melittin despite the fact that all three treatments have similar IC₅₀ values. This could be due to the different modes of action. Some modes of action, such as a drug causing competitive inhibition in a specific enzyme, cause slower increases in activity compared to a drug that permeabilizes cell membranes at low concentrations.

Planktonic *C. albicans* cells were exposed to Os at the IC₂₅, IC₅₀ and IC₇₅ and their ultrastructure was evaluated with SEM and TEM. AmpB was used as a positive control as its effects on *C. albicans* have been well-described (Pfaller and Diekema, 2007). With SEM the control cells have a typical oval shape and a smooth outer surface that represents the typical extracellular morphology of *C. albicans* (Figure 3.4). With TEM, *C. albicans* cells have a regular rounded shape with a clearly defined plasma membrane and cell wall with fibrils (Figure 3.5).

At the IC₂₅ of AmpB the cell shape is irregular, and at the IC₅₀ small evenly dispersed EV or similar structures are present on the cell wall. Pits and bud scars are also present with signs of extravasation of cellular contents. At a higher concentration, IC₇₅, the cells are elongated, with a ruffled surface and filamentation occurring. Cells treated with AmpB appeared to have blebbing on the surface. As AmpB concentrations increase, cells seem to become more shrivelled and overall morphologies of cells become irregular compared to untreated control. This seems to correlate with results found in previous studies (Bastide *et al.*, 1982). As the main target of AmpB is the membranes of cells, specifically the ergosterol within membranes (Brajtburg *et al.*, 1990), it is likely that the presence of the small EV is due to the formation of ergosterol-AmpB extramembranous structures (Laprade *et al.*, 2016). Disruption of the membranes to the point where cell leakage occurs would also possibly lead to shrivelling of cells.

With TEM, AmpB appears to affect the cell morphology in a dose-dependent manner. With increasing concentrations, the cell shape changes from a regular round to ovoid to a sickled shape. Fibrils are absent and the thickness of the cell wall varies from thin to thick. Another observation was that there was an increase in the abundance of peroxisomes compared with untreated cells. Some studies have found that AmpB induces the production of excessive amounts of ROS (Mesa-Arango *et al.*, 2014, Sokol-Anderson *et al.*, 1986). The observed increase in peroxisomes may be the result of AmpB induced ROS production. Increased ROS also causes oxidative damage to proteins and membranes, and damage to cell membranes can result in dysfunction and increased permeability.

Following exposure to AmpB, the cell membrane became irregular while in some areas it was absent or detached from the cell wall. The organelles, such as vacuoles and nuclei, were localized at the concave surface. The nucleus appears to be fragmented and the nuclear membrane damage is similar to that observed in the cell membrane and other intracellular membrane structures.

The morphology of the cells were altered and elongated with the formation of germ tubes especially following exposure to the IC₅₀ and IC₇₅ of AmpB. Laprade *et al.* (2016) identified that AmpB induced *C. albicans* filamentation as a protection mechanism, where the formation of biofilms protects against AmpB induced cell death. Therefore, the formation of germ tubes as observed in Figure 3.3 may be a protective response to the effects of AmpB.

The effects of AmpB have been evaluated with SEM and TEM by Grela *et al.* (2019). The proposed mechanism was that AmpB binds to the cell walls and plasma membranes of mature *C. albicans* cells (blue layer) forming ergosterol-AmpB extramembranous bulk forms (Figure 4.1) or is located in the cell membrane and vacuoles. In the present study, exposure to the IC₅₀ of AmpB resulted in the formation of small EV. Grela *et al.* (2019) provided no information on the size of the extramembranous bulk structures and therefore it cannot be concluded that the identified EV are the extramembranous bulk structures. In the daughter cells AmpB is located in the cell wall and membrane and accumulates in the vacuoles (Grela *et al.*, 2019). In addition to filamentation, the formation of pores indicates that the cell wall and membrane integrity is compromised. With TEM Grela *et al.* (2019) reported that the formation of blebs and pores is associated with changes in the structure of the cell wall and membrane.

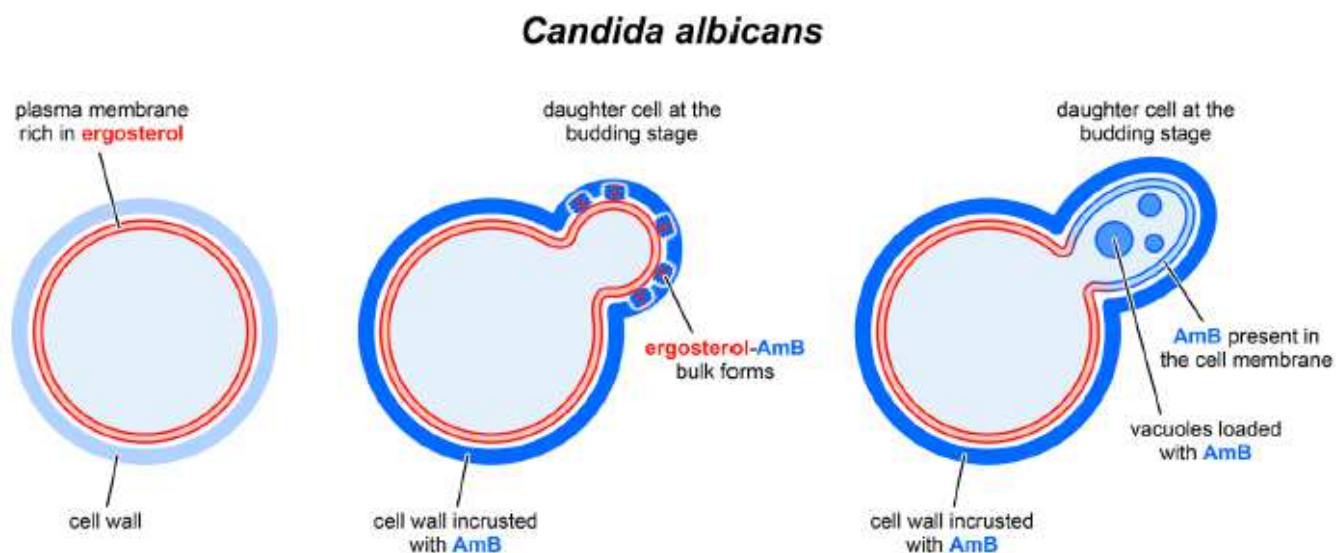


Figure 4.1: A model of activity of AmpB towards *C. albicans*. Cells of *C. albicans* (left) exposed to AmpB. AmpB binds to the cell walls of mature cells and prevents the formation of a functional cell wall of daughter cells at the budding stage. AmpB is located either in ergosterol-AmpB bulk extramembranous structures or binds into the cell membrane and penetrates into the cell (Grela *et al.*, 2019).

Cells treated with Os, observed with SEM, showed changes in overall structure, and effects were more severe when compared to cells treated with AmpB. Even at the IC₂₅ there were clear differences

in the overall shape of cells with cells adopting an elongated and curved shape. As concentrations of Os increase, indentations on the cell surface formed. This could indicate cell membrane permeabilization although it is unknown if this is a direct or an indirect effect, the latter due to binding of an intracellular target or interference with a biochemical process that results in cellular death.

At the IC_{75} of Os, the cells appeared flattened, as if the scaffolding within the cells (actin and other structural proteins) were affected (Brackley and Grantham, 2010). This could also be as result of the leakage or loss of the intracellular content. Cells treated with Os appeared very different to cells treated with AmpB, suggesting different modes of action. For example, no blebbing was seen on the surfaces of cells treated with Os. AmpB causes increased ROS and this leads to programmed cell death via yeast metacaspase *MCA1*. ROS production by Os does not lead to cell death (Table 1.1) further supporting a different mode of action. There were noticeably less peroxisomes visible in cells treated with Os compared to cells treated with AmpB, again implying that ROS production does not cause cellular death. Os appears to have a more severe effect on the overall integrity of the cell membranes of *C. albicans* cells compared with AmpB. This implies that Os is membrane targeting and supports the findings using liposomes (*Saccharomyces cerevisiae* polar extract and 30% ergosterol) (unpublished results) that Os targets cell membranes causing 50% leakage at 4 μ M. In the same study, melittin at 0.5 μ M caused 50% leakage. Finally, at higher concentrations of Os, the cell content appeared more electron dense and leakage of the cytoplasmic content or cellular shrinkage may account for this effect.

Observations from SEM and TEM images of planktonic *C. albicans* cells treated with Os showed some correlations such as damage to cell surfaces. Indentations of cell surfaces observed with SEM images correlate with the membrane damage visible in TEM images. This suggests that the cell membrane is one of the main targets of Os. Previous studies on Os showed that when testing its activity against bacteria, Os appears to mainly target that cell membranes as well (Taute, 2017, Mbuayama, 2016). Finally, there could be a correlation between the flattening of cells seen in SEM images and the granulation of the cytosol in TEM images. Both observations could be caused by the precipitation of intracellular structural proteins, such as actin filaments.

Prior to entering fungal cells peptides need to interact with the cell wall components (Han *et al.*, 2016). Two major polysaccharides present in the cell wall of *C. albicans* are laminarin and mannan. Peptides such as Gram-negative binding protein 3 (GNBP3) bind and thereby directly affect the cell wall. While others such as protonectin do not interact with the cell wall components but rather interact with the cell membrane and/or other intracellular targets (Mishima *et al.*, 2009, Wang *et al.*, 2015). To investigate this interaction Os was incubated in the presence of an excess of laminarin or mannan and then the antifungal activity was determined with the RDA (unpublished results). A reduction in the activity of Os was observed at 40 mg/mL of mannan or laminarin. This interaction was investigated in greater detail with ITC at concentrations used by Mishima *et al.* (2009). The control consisting of

EDTA and CaCO₃ gave a strong signal indicating 1:1 interaction (Henzl, 2009). At 1:20 and 1:40 molar ratios no detectable interactions between Os and laminarin or mannan respectively, were observed. Using the modified microbroth assay, activity of Os was evaluated in the presence of an excess of mannan or laminarin. At the same concentrations used for ITC, there were no changes in the inhibitory activity of Os. However, both laminarin and mannan at 20 mg/mL (relative ratio 1:400; Os:polysaccharide) decreased the inhibitory activity of Os against *C. albicans*.

No literature was found that evaluated the interaction between antimicrobial peptides and laminarin or mannan with ITC although several studies investigated the effects using the RDA. Studies on the interaction between carbohydrate binding proteins and carbohydrates provides important information on amino acid and secondary structural requirements for binding. Guillén *et al.* (2010) discussed the different carbohydrate-binding modules (CBM) found in hydrolytic enzymes with the function of breaking down polysaccharides. These CBMs are non-catalytic regions in the proteins that assist the protein in bringing the active site in close proximity with the hydrolysis sites. There are different classifications of CBMs, but in general there is a need for aromatic amino acids, such as tryptophan and tyrosine, to bind to the polysaccharide by means of van der Waals interactions. Another study by Miki *et al.* (2017) showed that the addition of tryptophan residues to the enzyme endo-1,3- β -glucanase improves its ability to bind to polysaccharides. The study also showed that certain charged amino acids, such as aspartic acid, are also essential for binding to polysaccharides. Finally, Gopalakrishnapai *et al.* (2006) described the importance of certain tryptophan and aspartate residues in the CBM of calreticulin, a membrane protein involved in the proper folding of glycoproteins. It is likely that Os is unable to bind to the cell wall due to the lack of tryptophan and aspartate residues required for binding. The secondary structure is also important for binding where a β -sheet conformation favours binding (Guillén *et al.*, 2010, Takahashi *et al.*, 2014). Simulations and circular dichroism analysis suggested that Os mainly contains α -helical regions and lacks the required β -sheet regions, and therefore based on its secondary structure will not bind.

With both the RDA and the modified microbroth dilution assays, binding between Os and 20 mg/mL laminarin or mannan decreased Os activity. Using the RDA, Jang *et al.* (2006) tested the interactions between the peptide di-K19Hc, a synthetic derivative of halocidin isolated from haemocytes of the tunicate, and laminarin and mannan. This peptide lost activity in 1 mg/mL laminarin but was unaffected by mannan. Compared with this peptide, Os generally binds laminarin and mannan poorly.

At higher concentrations, it seems that free laminarin and mannan has an effect on the activity of Os on planktonic *C. albicans* cells, but no effects were observed at lower concentrations. Takahashi *et al.* (2014) found that the binding of 0.2 mM insect β -1,3 glucan recognition protein to an excess laminarin (1-5 mM) at a molar ratio of >5 resulted in the formation of a soluble macro-complex stabilized by strong protein-protein and protein-carbohydrate interactions. This suggests that interactions between Os molecules and laminarin or mannan and the subsequent formation of a

macro-molecule complex limits the ability of Os to act as an antifungal peptide. This may account for the difference between the findings with ITC and the modified microbroth dilution assay. Of concern is that the concentrations of laminarin or mannan used in the RDA and microbroth dilution assay may not be physiologically relevant. Therefore, it is unlikely that Os binds to laminarin and mannan on the cell wall, however, other interactions such as electrostatic interactions between Os and the plasma membrane may play a role in Os binding to *C. albicans*.

Os has been shown to be membrane acting (Taute *et al.*, 2015, Mbuayama, 2016), and a further step in understanding this effect was to determine if Os causes membrane depolarization. Melittin was used as a control as this peptide causes membrane depolarization and its effects on membrane permeability and IC_{50} is similar to that of Os.

For melittin there was a linear increase in fluorescence while for Os a sigmoidal increase in fluorescence was observed. This indicated that for Os there is a critical threshold before membrane depolarization occurs. Melittin had a fluorescent signal of 1.0×10^7 at its IC_{50} whereas Os had a fluorescent signal lower than 1×10^6 at its IC_{50} , showing that melittin had more than ten-fold higher levels of fluorescence at its IC_{50} . Therefore, when compared to melittin, membrane depolarization is not a mode of action for Os (Park and Lee, 2010).

The ability of Os compared with melittin to cause permeabilization of liposomes (*S. cerevisiae* polar extract and 30% ergosterol) loaded with carboxyfluorescein was determined (unpublished results). Melittin and Os caused 50% liposome leakage at 0.5 μ M and 4 μ M respectively. With the SYTOX green uptake assay, melittin caused a linear increase in fluorescence while for Os there is a curve reaching a maximum of 70%. Interestingly, at the IC_{50} there is 50% fluorescence, indicating permeabilization without depolarization. Thus, Os does not cause membrane depolarization as a primary mode of action but rather permeabilizes the membrane, which then leads to membrane depolarization.

Other peptides in literature, such as arenicin-1 (a 21-residue peptide which was derived from *Arenicola marina*) and APP (a 20-residue peptide that was derived from an amphipathic α -helical cell-penetrating peptide ppTG20), showed the ability to cause membrane permeabilization in *Candida* species at sub-inhibitory concentrations (Li *et al.*, 2016, Park and Lee, 2009). It is important to note that in these studies, both peptides also caused membrane permeabilization at the same concentrations they caused membrane depolarization. This could indicate that peptides require the ability to cause membrane permeabilization in order to depolarize the membrane.

The final objective was to evaluate the effect of Os on the vacuoles of *C. albicans* evaluated with flow cytometry and CLSM using 5-FAM labelled Os in combination with the vacuole stain, CTB-CMAC. 5-FAM-Penetratin was used as a positive control as numerous studies have shown its ability to penetrate bacterial and fungal cell walls and plasma membranes (Gong and Karlsson, 2017, Alves *et*

al., 2011). Flow cytometry provided quantitative data on the effect of a large number of cells while CLSM provided specific information on intracellular localisation.

Cells treated with 5-FAM-penetratin showed strong positive fluorescence for 5-FAM with a low percentage of the cell population being positive for both 5-FAM-penetratin and CTB-CMAC. This indicated at the concentration evaluated (10 μM), 5-FAM-penetratin enters planktonic *C. albicans* cells and accumulates in the cytoplasm, breaking down intracellular membranes non-specifically. As described by Gong and Karlsson (2017), the decrease of CTB-CMAC fluorescence in combination with the increase of 5-FAM fluorescence is a good indicator that the peptide is breaking down intracellular membranous structures, such as the vacuoles.

Cells treated with 0.5 μM Os showed a strong fluorescent signal for both 5-FAM-Os and CTB-CMAC. At 6.3 μM there is a decrease in fluorescence for CTB-CMAC and the percentage of cells positive only for 5-FAM-Os alone is increased. This indicated that at higher concentrations, Os functions similar to penetratin by entering the cytosol and breaking down intracellular membranes non-specifically. This correlates with results seen with TEM where intracellular membranes, such as the nuclear membrane, were damaged. Cells treated with a lower concentration of 5-FAM Os (0.5 μM , IC_{25} of unlabelled Os) have higher signals of CTB-CMAC compared to cells treated with higher concentrations of Os (6.3 μM , IC_{75} of unlabelled Os). This further supports the membrane targeting effects of Os.

CLSM images showed complete staining with 5-FAM-penetratin with no staining of the nucleus. The amount of visible CTB-CMAC in vacuoles was also lower compared with untreated cells. These findings correlate with results from flow cytometry and were similar to the findings of Gong and Karlsson (2017) that also found that following exposure, strong 5-FAM-penetratin staining was observed with little CTB-CMAC staining.

At 0.5 μM , Os mostly localized on the cell membrane and staining of nuclei was observed. The latter confirms the findings of Taute (2017) that identified DNA as a potential target evaluated with the fluorescent intercalator displacement assay using pBR 322 vector from *E. coli*. CTB-CMAC staining of the vacuoles was also observed. At 6.3 μM all staining was intracellular and the vacuole staining was reduced. This effect was similar to the effect observed by Gong and Karlsson (2017), for penetratin, pVEC and SynB where at low concentrations there is both vacuole and 5-FAM-positive cells but with increasing concentrations the percentage of vacuole and 5-FAM positive cells decreases and the percentage of 5-FAM-positive cells increases. The proposed mechanism is that yeast vacuoles are necessary for homeostasis and the loss of vacuoles can lead to toxicity and cell death. Therefore, cell membrane staining and subsequent localisation to the cytoplasm was associated with a reduction in vacuolar staining indicating that Os is membrane targeting resulting the loss of vacuoles leading to cell death.

Previous studies on peptides such as MAP (synthetic, highly amphiphilic model peptide), TP-10 (fragment of transportan), hCT (derivative of calcitonin), SynB (derivative of the antimicrobial peptide protegrin), and PAF26 (hexapeptide with antimicrobial activity), have identified that these peptides are cell penetrating peptides that tend to localize in the lysosomes of mammalian cells with energy-dependent uptake (Drin *et al.*, 2003, Soomets *et al.*, 2000, Oehlke *et al.*, 1998, López-García *et al.*, 2002, Muñoz *et al.*, 2012).

The ability of a peptide to enter *C. albicans* cells is highly dependent on its hydrophobicity and net positive charge (Gong *et al.*, 2019). More specifically positive net charge has a bigger influence than hydrophobicity, but generally low hydrophobicity is associated with higher levels of vacuolar localisation and energy-dependent uptake. Penetratin has a positive net charge of +6, with an overall hydrophobicity of 33.46 (determined with Thermofisher Scientific peptide analyser software), uptake was not endocytosis dependent and the proposed mechanism was by micropinocytosis, direct translocation/pore formation (Gong and Karlsson, 2017). Os has a positive net charge of +6, overall hydrophobicity of 20.96 and uptake was via endocytosis, nuclear localisation occurred at a concentration lower than the IC₅₀, but at concentrations above the IC₅₀ membrane effects resulted in the loss of intracellular membrane integrity.

5 Conclusion and future perspectives

The activity of Os could not be determined using a standard microbroth dilution assay due to it losing activity in complex media, such as RPMI. A modified version of the microbroth dilution assay was developed to test Os against planktonic *C. albicans*. Os showed activity against planktonic *C. albicans* cells using the modified microbroth dilution assay with a relatively low IC₅₀ value. Controls, such as AmpB and melittin, were also tested under these conditions and were comparable to the activity of Os. Although planktonic *C. albicans* cells are not representative of fungal infections that are usually biofilms, this method allows rapid screening of peptide activity.

This method is ideal for the rapid screening of salt sensitive AMPs. Once identified, lead peptides can be modified to be more resistant to high salt concentrations and proteolysis (Balkovec *et al.*, 2014, Bouffard *et al.*, 1994). This can be achieved by for example using D-enantiomers of amino acids, and making the peptide more hydrophobic by adding hydrophobic amino acids, such as tryptophan tagging at the N- or C-terminal (Ramafoko, 2018). Yu *et al.* (2011) showed that by replacing tryptophan and histidine residues in AMPs with bigger residues, such as β -naphthylalanine and β -(4,4'-biphenyl)alanine, the activity of these peptides in high salt concentrations is increased. If a low IC₅₀ is obtained the AMP can be further evaluated for activity using the standard microbroth dilution assay.

When comparing the effects of Os and AmpB with SEM and TEM on the cell membrane, it appears that Os has a more drastic and non-specific effect on the cell wall and membrane. AmpB is known to target ergosterol in the membrane, leading to destabilization and finally the breakdown of the cell membrane. Os seems to break down the membrane in a more direct manner and may lead to the formation of membrane lipid micelles resulting in large pores and cell rupture. Additionally, there is a significant amount of extracellular blebbing seen on cells treated with Os (Figure 3.3). TEM images of *C. albicans* cells treated with Os also showed large groups of peroxisomes and granulation within the cytosol. The formation of peroxisomes is most like due to Os affecting mitochondria, possibly breaking down mitochondrial membranes. Granulation within the cytosol is most likely precipitation of intracellular proteins but more experimentation is required to confirm this.

Several models have been proposed to explain the membrane acting effects of AMPs. The extent and the size of pore formation and possible mechanism can be determined using dextran of different sizes labelled with fluorescein. The size of the labelled dextran that enters treated cells will provide an indication of pore size and possibly provide information on the mode of action (Moore *et al.*, 2018).

Os does not bind laminarin or mannan at physiological concentrations and therefore does not disrupt the integrity of the cell wall through binding of these components. Very high concentrations of cell wall components, much higher than what would naturally be found in a suspension of planktonic *C.*

albicans cells, were required to affect the activity of Os. The ITC results also showed no detectable interactions between Os and the cell wall components of *C. albicans* in buffer solution.

Using liposomal environments or whole cells (Lakshminarayanan *et al.*, 2014, Alves *et al.*, 2011), the ability of Os to bind to the cell wall and membrane can be determined more accurately. Additionally, Os could be modified to more closely resemble CBM's, such as adding tryptophan and aspartate residues at key points in the sequence, so that Os can better bind cell wall components (Miki *et al.*, 2017). Os can also be tested for interactions with ergosterol, an important component in the stabilizing of the plasma membranes of fungi. A large group of antifungal drugs, known as polyenes, are already known to target ergosterol in the plasma membranes of fungal cells (Campoy and Adrio, 2017). By using antagonism between azoles, a group of drugs known to inhibit the production of ergosterol in fungal cells, and polyenes, the ability of Os also to bind ergosterol can be determined. If Os shows the same antagonism as seen between AmpB and an azole, it could indicate that ergosterol is needed for the activity of Os (Vazquez *et al.*, 1996).

Os does not induce membrane depolarization. If membrane depolarization is a primary mechanism associated with permeabilization, depolarization would occur at lower concentrations. In general, antimicrobial drugs that are known to cause membrane depolarization target specific membrane proteins responsible for maintaining polarized cell membranes (Liu *et al.*, 2015). This further supports the finding that Os is predominantly membrane targeting.

To confirm that membrane depolarization is not a primary mode of action more specific methods are required, which include investigating the interactions between the peptide and specific membrane proteins responsible for membrane depolarization (Wenzel *et al.*, 2014). Also, the ability of Os to inhibit the intracellular synthesis of membrane proteins required for membrane polarization (Graf *et al.*, 2017) can be investigated.

The CLSM images indicated that Os is able to penetrate *C. albicans* cell membranes, especially at higher concentrations. At lower concentrations, Os seems to primarily localize within the cell membranes of *C. albicans* and in some cells, Os is concentrated in what appears to be the nuclei, confirming previous findings where it was shown that Os interacts with double-stranded DNA (Taute, 2017). To confirm this observation DNA can be isolated from *C. albicans* and 5-FAM-Os can be used to determine the binding ability to fungal DNA with gel electrophoresis. Some staining of the vacuoles is observed. At higher concentrations, Os appears to localize non-specifically. With flow cytometry, the loss of vacuole staining at concentrations lower than the IC₅₀ was confirmed.

Further investigation is required to better understand the mechanism of Os uptake. A previous study by Li *et al.* (2019) on a peptide known as CGA-N9, a derivative of human chromogranin, used sodium azide (NaN₃) to show that the peptide was able to enter cells in an energy independent manner. Using a similar strategy Os uptake into cells was found to be via endocytosis (unpublished results). Using

the selective inhibitors, 5-(*N*-ethyl-*N*-isopropyl)-amiloride, cytochalasin D and heparin the uptake of Os via micropinocytosis can be determined. Gong and Karlsson (2017) reported that the uptake of peptides could be either energy-dependent or energy-independent. AMPs that cause membrane permeabilization generally enter fungal cells in an energy-independent manner. This means that Os most likely enters *C. albicans* in an energy-dependent manner at lower concentrations. As the concentration of Os increases and it starts to permeabilize the membranes of cells, it starts to enter cells primarily through energy-independent pathways. This can be investigated further by using time- and concentration-dependant studies in the presence of NaN₃.

In conclusion, this study has found that the main mode of action of Os in planktonic *C. albicans* cells is firstly to bind to the cell membrane, then to translocate and possibly bind DNA, with no depolarization occurring. At a higher concentration above the IC₅₀, Os accumulates in the cytoplasm and destruction of membranes including that of vacuoles leads to cell death. What is possibly the most interesting aspect of Os is its selectivity for bacterial and fungal plasma membranes, with limited effects on the cell membrane of mammalian cells (Taute, 2017). Therefore, it will be important in future studies to undertake detailed studies regarding the interaction between Os and the negative components of the cell wall and membranes including proteins or specific lipid polar head groups with techniques such as molecular dynamics (Manzo *et al.*, 2019).

6 References

- Akhtar, K., Khan, S. A., Khan, S. B. & Asiri, A. M. 2018. Scanning Electron Microscopy: Principle and Applications in Nanomaterials Characterization. *Handbook of Materials Characterization*.
- Alves, I. D., Bechara, C., Walrant, A., Zaltsman, Y., Jiao, C. Y. & Sagan, S. 2011. Relationships between membrane binding, affinity and cell internalization efficacy of a cell-penetrating peptide: penetratin as a case study. *PLoS One*, 6, e24096.
- Arino, J., Ramos, J. & Sychrová, H. 2010. Alkali metal cation transport and homeostasis in yeasts. *Microbiology and Molecular Biology Reviews*, 74, 95-120.
- Balkovec, J. M., Hughes, D. L., Masurekar, P. S., Sable, C. A., Schwartz, R. E. & Singh, S. B. 2014. Discovery and development of first in class antifungal caspofungin (CANCIDAS®)—A case study. *Natural Product Reports*, 31, 15-34.
- Bastide, M., Jouvert, S. & Bastide, J.-M. 1982. A comparison of the effects of several antifungal imidazole derivatives and polyenes on *Candida albicans*: an ultrastructural study by scanning electron microscopy. *Canadian Journal of Microbiology*, 28, 1119-1126.
- Beards, G. (2020). File:Electron Microscope.png - Wikimedia Commons. [online] Commons.wikimedia.org. Available at: https://commons.wikimedia.org/wiki/File:Electron_Microscope.png [Accessed 18 Feb. 2020].
- Bouffard, F. A., Zambias, R. A., Dropinski, J. F., Balkovec, J. M., Hammond, M. L., Abruzzo, G. K., Bartizal, K. F., Marrinan, J. A. & Kurtz, M. B. 1994. Synthesis and antifungal activity of novel cationic pneumocandin Bo derivatives. *Journal of Medicinal Chemistry*, 37, 222-225.
- Bozzola, J. J. & Russell, L. D. 1999. *Electron microscopy: principles and techniques for biologists*, Jones & Bartlett Learning.
- Brackley, K. I. & Grantham, J. 2010. Subunits of the chaperonin CCT interact with F-actin and influence cell shape and cytoskeletal assembly. *Experimental Cell Research*, 316, 543-553.
- Brajtburg, J., Powderly, W. G., Kobayashi, G. S. & Medoff, G. 1990. Amphotericin B: current understanding of mechanisms of action. *Antimicrobial agents and Chemotherapy*, 34, 183-188.
- Brogden, K. A. 2005. Antimicrobial peptides: pore formers or metabolic inhibitors in bacteria? *Nature Reviews Microbiology*, 3, 238-250.
- Brune, M. E., Fey, T. A., Brioni, J. D., Sullivan, J. P., Williams, M., Carroll, W. A., Coghlan, M. J. & Gopalakrishnan, M. 2002. (-)-(9S)-9-(3-Bromo-4-fluorophenyl)-2, 3, 5, 6, 7, 9-hexahydrothieno [3, 2-b] quinolin-8 (4H)-one 1, 1-dioxide (A-278637): a novel ATP-sensitive potassium channel opener efficacious in suppressing urinary bladder contractions. II. in vivo characterization. *Journal of Pharmacology and Experimental Therapeutics*, 303, 387-394.
- Campoy, S. & Adrio, J. L. 2017. Antifungals. *Biochemical Pharmacology*, 133, 86-96.
- Castillo-Hair, S. 2016. *FlowCal: Software for Analysis and Calibration of Flow Cytometry Data* [Online]. Benchling: [online] Benchling. Available:

<https://www.benchling.com/2018/11/06/flowcal-software-for-analysis-and-calibration-of-flow-cytometry-data/> [Accessed 23 Jan 2020].

- Chaffin, W. L. 2008. *Candida albicans* cell wall proteins. *Microbiology and Molecular Biology Reviews*, 72, 495-544.
- Chung, P. Y. & Khanum, R. 2017. Antimicrobial peptides as potential anti-biofilm agents against multidrug-resistant bacteria. *Journal of Microbiology, Immunology and Infection*, 50, 405-410.
- Desig.kristinejaynephography.com. (2020). how does light travel through a microscope - Desig.kristinejaynephography.com. [online] Available at: <http://desig.kristinejaynephography.com/how-does-light-travel-through-a-microscope/> [Accessed 5 Mar. 2020].
- Drin, G., Cottin, S., Blanc, E., Rees, A. R. & Temsamani, J. 2003. Studies on the internalization mechanism of cationic cell-penetrating peptides. *Journal of Biological Chemistry*, 278, 31192-31201.
- Elicharova, H. & Sychrova, H. 2013. Fluconazole treatment hyperpolarizes the plasma membrane of *Candida* cells. *Medical Mycology*, 51, 785-794.
- Feng, Q., Li, N.-Q. & Jiang, Y.-Y. 1997. Electrochemical studies of porphyrin interacting with DNA and determination of DNA. *Analytica Chimica Acta*, 344, 97-104.
- Fischer, A. H., Jacobson, K. A., Rose, J. & Zeller, R. 2008. Preparation of slides and coverslips for microscopy. *Cold Spring Harbor Protocols*, 2008, pdb. prot4988.
- Freire, E., Mayorga, O. L. & Straume, M. 1990. Isothermal titration calorimetry. *Analytical Chemistry*, 62, 950A-959A.
- Ganz, T., Selsted, M. E. & Lehrer, R. I. 1990. Defensins. *European Journal of Haematology*, 44, 1-8.
- Garcia-Rubio, R., De Oliveira, H. C., Rivera, J. & Trevijano-Contador, N. 2019. The Fungal Cell Wall: *Candida*, *Cryptococcus*, and *Aspergillus* Species. *Frontiers in Microbiology*, 10, 2993.
- Gillespie And, J. P., Kanost, M. R. & Trenczek, T. 1997. Biological mediators of insect immunity. *Annual Review of Entomology*, 42, 611-643.
- Gong, Z., Doolin, M. T., Adhikari, S., Stroka, K. M. & Karlsson, A. J. 2019. Role of charge and hydrophobicity in translocation of cell-penetrating peptides into *Candida albicans* cells. *AICHE Journal*, 65, e16768.
- Gong, Z. & Karlsson, A. J. 2017. Translocation of cell-penetrating peptides into *Candida* fungal pathogens. *Protein Science*, 26, 1714-1725.
- Gopalakrishnapai, J., Gupta, G., Karthikeyan, T., Sinha, S., Kandiah, E., Gemma, E., Oscarson, S. & Suroliya, A. 2006. Isothermal titration calorimetric study defines the substrate binding residues of calreticulin. *Biochemical and Biophysical Research Communications*, 351, 14-20.

- Graf, M., Mardirossian, M., Nguyen, F., Seefeldt, A. C., Guichard, G., Scocchi, M., Innis, C. A. & Wilson, D. N. 2017. Proline-rich antimicrobial peptides targeting protein synthesis. *Natural Product Reports*, 34, 702-711.
- Grela, E., Zdybicka-Barabas, A., Pawlikowska-Pawlega, B., Cytrynska, M., Wlodarczyk, M., Grudzinski, W., Luchowski, R. & Gruszecki, W. I. 2019. Modes of the antibiotic activity of amphotericin B against *Candida albicans*. *Scientific Reports*, 9, 1-10.
- Guillén, D., Sánchez, S. & Rodríguez-Sanoja, R. 2010. Carbohydrate-binding domains: multiplicity of biological roles. *Applied Microbiology and Biotechnology*, 85, 1241-1249.
- Gulati, M. & Nobile, C. J. 2016. *Candida albicans* biofilms: development, regulation, and molecular mechanisms. *Microbes and Infections*, 18, 310-321.
- Han, J., Jyoti, M. A., Song, H. Y. & Jang, W. S. 2016. Antifungal Activity and Action Mechanism of Histatin 5-Halocidin Hybrid Peptides against *Candida ssp.* *PLoS One*, 11, e0150196.
- Hancock, R. E. W. & Diamond, G. 2000. The role of cationic antimicrobial peptides in innate host defences. *Trends in Microbiology*, 8, 402-409.
- Henzl, M. T. 2009. Characterization of parvalbumin and polcalcin divalent ion binding by isothermal titration calorimetry. *Methods in Enzymology*, 455, 259-297.
- Ismail, N. O., Odendaal, C., Serem, J. C., Strömstedt, A. A., Bester, M. J., Sayed, Y., Neitz, A. W. & Gaspar, A. R. 2019. Antimicrobial function of short amidated peptide fragments from the tick-derived OsDef2 defensin. *Journal of Peptide Science*, 25, e3223.
- Jang, W. S., Kim, H. K., Lee, K. Y., Kim, S. A., Han, Y. S. & Lee, I. H. 2006. Antifungal activity of synthetic peptide derived from halocidin, antimicrobial peptide from the tunicate, *Halocynthia aurantium*. *FEBS Lett*, 580, 1490-1496.
- Johnston, D. A., Eberle, K. E., Sturtevant, J. E. & Palmer, G. E. 2009. Role for endosomal and vacuolar GTPases in *Candida albicans* pathogenesis. *Infection and Immunity*, 77, 2343-2355.
- Kanakamedala, K. 2019. Characterization of tin-oxide (SnO₂-Ni) based sensors. *International Journal of Emerging Technology and Advanced Engineering*, 9, 91-100.
- Klis, F., Groot, P. D. & Hellingwerf, K. 2001. Molecular organization of the cell wall of *Candida albicans*. *Medical Mycology*, 39, 1-8.
- Lafleur, M. D., Kumamoto, C. A. & Lewis, K. 2006. *Candida albicans* biofilms produce antifungal-tolerant persister cells. *Antimicrobial Agents and Chemotherapy*, 50, 3839-3846.
- Lakshminarayanan, R., Liu, S., Li, J., Nandhakumar, M., Aung, T. T., Goh, E., Chang, J. Y., Saraswathi, P., Tang, C., Safie, S. R., Lin, L. Y., Riezman, H., Lei, Z., Verma, C. S. & Beuerman, R. W. 2014. Synthetic multivalent antifungal peptides effective against fungi. *PLoS One*, 9, e87730.
- Laprade, D. J., Brown, M. S., Mccarthy, M. L., Ritch, J. J. & Austriaco, N. 2016. Filamentation protects *Candida albicans* from amphotericin B-induced programmed cell death via a mechanism involving the yeast metacaspase, MCA1. *Microbial Cell*, 3, 285-292.

- Levy, S. B. 2002. Factors impacting on the problem of antibiotic resistance. *Journal of Antimicrobial Chemotherapy*, 49, 25-30.
- Li, L., Sun, J., Xia, S., Tian, X., Cheserek, M. J. & Le, G. 2016. Mechanism of antifungal activity of antimicrobial peptide APP, a cell-penetrating peptide derivative, against *Candida albicans*: intracellular DNA binding and cell cycle arrest. *Applied Microbiology and Biotechnology*, 100, 3245-3253.
- Li, R., Chen, C., Zhu, S., Wang, X., Yang, Y., Shi, W., Chen, S., Wang, C., Yan, L. & Shi, J. 2019. CGA-N9, an antimicrobial peptide derived from chromogranin A: direct cell penetration of and endocytosis by *Candida tropicalis*. *Biochemistry Journal J*, 476, 483-497.
- Liu, S., Hou, Y., Liu, W., Lu, C., Wang, W. & Sun, S. 2015. Components of the calcium-calcineurin signaling pathway in fungal cells and their potential as antifungal targets. *Eukaryotic Cell*, 14, 324-334.
- López-García, B., Pérez-Payá, E. & Marcos, J. F. 2002. Identification of novel hexapeptides bioactive against phytopathogenic fungi through screening of a synthetic peptide combinatorial library. *Applied and Environmental Microbiology*, 68, 2453-2460.
- Mahlapuu, M., Hakansson, J., Ringstad, L. & Bjorn, C. 2016. Antimicrobial Peptides: An Emerging Category of Therapeutic Agents. *Frontiers in Cellular and Infection Microbiology*, 6, 194-206.
- Malan, M., Serem, J. C., Bester, M. J., Neitz, A. W. & Gaspar, A. R. 2016. Anti-inflammatory and anti-endotoxin properties of peptides derived from the carboxy-terminal region of a defensin from the tick *Ornithodoros savignyi*. *Journal of Peptide Science*, 22, 43-51.
- Manzo, G., Ferguson, P. M., Gustilo, V. B., Hind, C. K., Clifford, M., Bui, T. T., Drake, A. F., Atkinson, R. A., Sutton, J. M., Batoni, G., Lorenz, C. D., Phoenix, D. A. & Mason, A. J. 2019. Minor sequence modifications in temporin B cause drastic changes in antibacterial potency and selectivity by fundamentally altering membrane activity. *Scientific Reports*, 9, 1385-1401.
- Maurya, I. K., Pathak, S., Sharma, M., Sanwal, H., Chaudhary, P., Tupe, S., Deshpande, M., Chauhan, V. S. & Prasad, R. 2011. Antifungal activity of novel synthetic peptides by accumulation of reactive oxygen species (ROS) and disruption of cell wall against *Candida albicans*. *Peptides*, 32, 1732-1740.
- Mbuayama, K. R. 2016. Antifungal properties of peptides derived from a defensin from the tick *Ornithodoros savignyi*. Masters, University of Pretoria.
- Mesa-Arango, A. C., Trevijano-Contador, N., Román, E., Sánchez-Fresneda, R., Casas, C., Herrero, E., Argüelles, J. C., Pla, J., Cuenca-Estrella, M. & Zaragoza, O. 2014. The production of reactive oxygen species is a universal action mechanism of amphotericin B against pathogenic yeasts and contributes to the fungicidal effect of this drug. *Antimicrobial Agents and Chemotherapy*, 58, 6627-6638.
- Miki, A., Inaba, S., Maruno, T., Kobayashi, Y. & Oda, M. 2017. Tryptophan introduction can change β -glucan binding ability of the carbohydrate-binding module of endo-1, 3- β -glucanase. *Bioscience, Biotechnology, and Biochemistry*, 81, 951-957.

- Mishima, Y., Quintin, J., Amanianda, V., Kellenberger, C., Coste, F., Clavaud, C., Hetru, C., Hoffmann, J. A., Latgé, J.-P., Ferrandon, D. & Roussel, A. 2009. The N-terminal domain of drosophila gram-negative binding protein 3 (GNBP3) defines a novel family of fungal pattern recognition receptors. *Journal of Biological Chemistry*, 284, 28687-28697.
- Mojsoska, B. & Jenssen, H. 2015. Peptides and peptidomimetics for antimicrobial drug design. *Pharmaceuticals*, 8, 366-415.
- Moore, J., Rajasekaran, K., Cary, J. W. & Chlan, C. 2018. Mode of Action of the Antimicrobial Peptide D4E1 on *Aspergillus flavus*. *International Journal of Peptide Research and Therapeutics*, 25, 1135-1145.
- Mukherjee, P. K., Chandra, J., Kuhn, D. M. & Ghannoum, M. A. 2003. Mechanism of fluconazole resistance in *Candida albicans* biofilms: phase-specific role of efflux pumps and membrane sterols. *Infection and Immunity*, 71, 4333-4340.
- Muñoz, A., Marcos, J. F. & Read, N. D. 2012. Concentration-dependent mechanisms of cell penetration and killing by the de novo designed antifungal hexapeptide PAF26. *Molecular Microbiology*, 85, 89-106.
- Nakajima, Y., Ogihara, K., Taylor, D. & Yamakawa, M. 2003. Antibacterial hemoglobin fragments from the midgut of the soft tick, *Ornithodoros moubata* (Acari: Argasidae). *Journal of Medical Entomology*, 40, 78-81.
- Nevidalova, H., Michalcova, L. & Glatz, Z. 2018. In-depth insight into the methods of plasma protein-drug interaction studies: Comparison of capillary electrophoresis-frontal analysis, isothermal titration calorimetry, circular dichroism and equilibrium dialysis. *Electrophoresis*, 39, 581-589.
- Nobile, C. J. & Johnson, A. D. 2015. *Candida albicans* Biofilms and Human Disease. *Annual Review of Microbiology*, 69, 71-92.
- Oehlke, J., Scheller, A., Wiesner, B., Krause, E., Beyermann, M., Klausch, E., Melzig, M. & Bienert, M. 1998. Cellular uptake of an α -helical amphipathic model peptide with the potential to deliver polar compounds into the cell interior non-endocytically. *Biochimica et Biophysica Acta (BBA)-Biomembranes*, 1414, 127-139.
- Orlov, D. S., Nguyen, T. & Lehrer, R. I. 2002. Potassium release, a useful tool for studying antimicrobial peptides. *Journal of Microbiological Methods*, 49, 325-328.
- Palmer, G. E. 2011. Vacuolar trafficking and *Candida albicans* pathogenesis. *Communicative and Integrative Biology*, 4, 240-2.
- Palmer, G. E., Cashmore, A. & Sturtevant, J. 2003. *Candida albicans* VPS11 is required for vacuole biogenesis and germ tube formation. *Eukaryotic Cell*, 2, 411-421.
- Park, C. & Lee, D. G. 2009. Fungicidal effect of antimicrobial peptide arenicin-1. *Biochim Biophysica Acta*, 1788, 1790-1796.
- Park, C. & Lee, D. G. 2010. Melittin induces apoptotic features in *Candida albicans*. *Biochemical and Biophysical Research Communications*, 394, 170-172.

- Park, S. C., Park, Y. & Hahm, K. S. 2011. The role of antimicrobial peptides in preventing multidrug-resistant bacterial infections and biofilm formation. *International Journal of Molecular Sciences*, 12, 5971-92.
- Petersen, S. V., Thiel, S. & Jensenius, J. C. 2001. The mannan-binding lectin pathway of complement activation: biology and disease association. *Molecular Immunology*, 38, 133-149.
- Pfaller, M. A. & Diekema, D. J. 2007. Epidemiology of invasive candidiasis: a persistent public health problem. *Clinical Microbiology Reviews*, 20, 133-163.
- Prinsloo, L., Naidoo, A., Serem, J., Taute, H., Sayed, Y., Bester, M., Neitz, A. & Gaspar, A. 2013. Structural and functional characterization of peptides derived from the carboxy-terminal region of a defensin from the tick *Ornithodoros savignyi*. *Journal of Peptide Science*, 19, 325-332.
- Ramafoko, S. A. 2018. The effect of tryptophan end-tagging on the function of antimicrobial peptide, Os-C, derived from the tick *Ornithodoros savignyi*. MSc Biochemistry, University of Pretoria.
- Ramos, J., Ariño, J. & Sychrová, H. 2011. Alkali-metal-cation influx and efflux systems in nonconventional yeast species. *FEMS Microbiology Letters*, 317, 1-8.
- Rane, H. S., Bernardo, S. M., Raines, S. M., Binder, J. L., Parra, K. J. & Lee, S. A. 2013. *Candida albicans* VMA3 is necessary for V-ATPase assembly and function and contributes to secretion and filamentation. *Eukaryotic Cell*, 12, 1369-1382.
- Reimer, L. 2013. *Transmission electron microscopy: physics of image formation and microanalysis*, Springer.
- Rittner, K., Benavente, A., Bompard-Sorlet, A., Heitz, F., Divita, G., Bresseur, R. & Jacobs, E. 2002. New basic membrane-destabilizing peptides for plasmid-based gene delivery in vitro and in vivo. *Molecular Therapy*, 5, 104-114.
- Ruiz-Herrera, J., Elorza, M. V., Valentin, E. & Sentandreu, R. 2006. Molecular organization of the cell wall of *Candida albicans* and its relation to pathogenicity. *FEMS Yeast Research*, 6, 14-29.
- Salyers, A., Palmer, J. & Wilkins, T. 1977. Laminarinase (beta-glucanase) activity in Bacteroides from the human colon. *Applied and Environmental Microbiology*, 33, 1118-1124.
- Shapiro, H. M. 2005. *Practical flow cytometry*, John Wiley & Sons.
- Sokol-Anderson, M. L., Brajtburg, J. & Medoff, G. 1986. Amphotericin B-induced oxidative damage and killing of *Candida albicans*. *Journal of Infectious Diseases*, 154, 76-83.
- Soomets, U., Lindgren, M., Gallet, X., Hällbrink, M., Elmquist, A., Balaspiri, L., Zorko, M., Pooga, M., Bresseur, R. & Langel, Ü. 2000. Deletion analogues of transportan. *Biochimica et Biophysica Acta (BBA)-Biomembranes*, 1467, 165-176.
- Spring, K., Fellers, T. and Davidson, M. (2012). Olympus Microscopy Resource Center | Confocal Microscopy - Confocal Microscope Scanning Systems. [online] Olympus.magnet.fsu.edu. Available at: <http://olympus.magnet.fsu.edu/primer/techniques/confocal/confocalscanningsystems.html> [Accessed 18 Feb. 2020].

- Stotz, H. U., Thomson, J. & Wang, Y. 2014. Plant defensins. *Plant Signaling & Behavior*, 4, 1010-1012.
- Takahashi, D., Dai, H., Hiromasa, Y., Krishnamoorthi, R. & Kanost, M. R. 2014. Self-association of an insect β -1, 3-glucan recognition protein upon binding laminarin stimulates prophenoloxidase activation as an innate immune response. *Journal of Biological Chemistry*, 289, 28399-28410.
- Taute, H. 2017. The mode of action of the synthetic peptides Os and Os-C derived from the soft tick *Ornithodoros savignyi*. PhD Dissertation, University of Pretoria.
- Taute, H., Bester, M. J., Neitz, A. W. & Gaspar, A. R. 2015. Investigation into the mechanism of action of the antimicrobial peptides Os and Os-C derived from a tick defensin. *Peptides*, 71, 179-187.
- Taylor, D. 2006. Innate immunity in ticks: a review. *Journal of the Tick Society of Japan*, 15, 109-127.
- Testing, S. O. a. S. T. O. T. E. E. C. F. a. S. 2008. EUCAST definitive document EDef 7.1: method for the determination of broth dilution MICs of antifungal agents for fermentative yeasts. *Clinical Microbiology and Infection*, 14, 398-405.
- Toraya, S., Nagao, T., Norisada, K., Tuzi, S., Saitô, H., Izumi, S. & Naito, A. 2005. Morphological behavior of lipid bilayers induced by melittin near the phase transition temperature. *Biophysical Journal*, 89, 3214-3222.
- Troskie, A. M., Rautenbach, M., Delattin, N., Vosloo, J. A., Dathe, M., Cammue, B. P. & Thevissen, K. 2014. Synergistic activity of the tyrocidines, antimicrobial cyclodecapeptides from *Bacillus aneurinolyticus*, with amphotericin B and caspofungin against *Candida albicans* biofilms. *Antimicrobial Agents and Chemotherapy*, 58, 3697-3707.
- Van Der Goes Van Naters-Yasui, A. Purification and partial amino acid sequence of antibacterial peptides from the hemolymph of the soft tick, *Ornithodoros moubata* (Acari: Argasidae). Proceedings of the 3rd International Conference on Ticks and Tick-borne Pathogens: Into the 21st Century, Bratislava, Slovakia, 2000, 2000. Institute of Zoology, Slovak Academy of Sciences.
- Van Der Kraan, M. I., Van Marle, J., Nazmi, K., Groenink, J., Van 'T Hof, W., Veerman, E. C., Bolscher, J. G. & Nieuw Amerongen, A. V. 2005. Ultrastructural effects of antimicrobial peptides from bovine lactoferrin on the membranes of *Candida albicans* and *Escherichia coli*. *Peptides*, 26, 1537-1542.
- Vazquez, J. A., Arganoza, M. T., Vaishampayan, J. K. & Akins, R. A. 1996. In vitro interaction between amphotericin B and azoles in *Candida albicans*. *Antimicrobial Agents and Chemotherapy*, 40, 2511-2516.
- Veses, V., Richards, A. & Gow, N. A. 2008. Vacuoles and fungal biology. *Current Opinion in Microbiology*, 11, 503-510.
- Wang, K., Dang, W., Xie, J., Zhu, R., Sun, M., Jia, F., Zhao, Y., An, X., Qiu, S., Li, X., Ma, Z., Yan, W. & Wang, R. 2015. Antimicrobial peptide protonectin disturbs the membrane integrity and induces ROS production in yeast cells. *Biochimica et Biophysica Acta (BBA) - Biomembranes*, 1848, 2365-2373.

- Wenzel, M., Chiriac, A. I., Otto, A., Zweytick, D., May, C., Schumacher, C., Gust, R., Albada, H. B., Penkova, M., Kramer, U., Erdmann, R., Metzler-Nolte, N., Straus, S. K., Bremer, E., Becher, D., Brotz-Oesterhelt, H., Sahl, H. G. & Bandow, J. E. 2014. Small cationic antimicrobial peptides delocalize peripheral membrane proteins. *Proceedings of the National Academy of Sciences of the United States of America*, 111, E1409-18.
- Witebsky, F. G., Maclowry, J. & French, S. 1979. Broth dilution minimum inhibitory concentrations: rationale for use of selected antimicrobial concentrations. *Journal of Clinical Microbiology*, 9, 589-595.
- Wong, J. H., Xia, L. & Ng, T. 2007. A review of defensins of diverse origins. *Current Protein and Peptide Science*, 8, 446-459.
- Yan, J., Yuan, S. S., Jiang, L. L., Ye, X. J., Ng, T. B. & Wu, Z. J. 2015. Plant antifungal proteins and their applications in agriculture. *Applied Microbiology and Biotechnology*, 99, 4961-4981.
- Yeung, A. T., Gellatly, S. L. & Hancock, R. E. 2011. Multifunctional cationic host defence peptides and their clinical applications. *Cellular and Molecular Life Sciences*, 68, 2161-2176.
- Yu, H. Y., Tu, C. H., Yip, B. S., Chen, H. L., Cheng, H. T., Huang, K. C., Lo, H. J. & Cheng, J. W. 2011. Easy strategy to increase salt resistance of antimicrobial peptides. *Antimicrobial Agents and Chemotherapy*, 55, 4918-4921.
- Zasloff, M. 2002. Antimicrobial peptides of multicellular organisms. *Nature*, 415, 389-395.
- Zeya, H. & Spitznagel, J. K. 1963. Antibacterial and enzymic basic proteins from leukocyte lysosomes: separation and identification. *Science*, 142, 1085-1087.
- Zoric, N., Kosalec, I., Tomic, S., Bobnjarić, I., Jug, M., Vlajnić, T. & Vlajnić, J. 2017. Membrane of *Candida albicans* as a target of berberine. *BMC Complementary and Alternative Medicine*, 17, 268-278.